

Recent Advances and Perspectives in Microfluidics-Based Single-Cell Biosensing Techniques

Jiacheng He, Ayoola T. Brimmo, Mohammad A. Qasaimeh, Pengyu Chen, and Weiqiang Chen*

Single-cell analyses of secretory proteins are essential to fully understand cellular functional heterogeneity and unravel the underlying mechanisms of intercellular signaling and interactions. Retrieving dynamic information of protein secretion at single-cell resolution reflects the precise, real-time functional states of individual cells in physiological processes. Such measurements remain very challenging in single-cell analysis, which requires highly integrated systems capable of performing on-chip single-cell isolation and subsequent real-time protein detection. Here, recent advances in microfluidics-based single-cell manipulation and emerging approaches for label-free single-cell biosensing are reviewed. The advantages and limitations of these technologies are summarized and challenges to establish the integrated microfluidic biosensing systems for real-time single-cell secretomics are discussed. Recent efforts on integrated platforms for on-chip single-cell protein assays are highlighted and some perspectives on future directions in this field are provided.

1. Introduction

Cellular analysis with accurate, in-depth information on cell characteristics, behaviors, and functions offers critical insights to modern biology and clinical sciences. Cell populations, as a whole, produce reliable biological responses through multi-level interplays among different cell types over varying time and length scales. Thus, cellular analysis can either be

performed at the system level to measure the average response from the entire cell population or at the single-cell level by revealing the hierarchical and interconnected attributes of the highly heterogeneous cell subsets. The former approach, including conventional enzyme-linked immunosorbent assays (ELISA), quantitative polymerase chain reaction (qPCR), and other common biological assays, do provide exceptional insights into life science and medical diagnosis.^[1–5] However, these methods obscure important information regarding the specific phenotypes and status of the cells, and fail to unravel the casual events and the basic nature of cellular interactions among the discriminated cell types. Conversely, lateral technologies, by enabling the investigation of cellular responses at a fine resolution of individual cells and their interactions over


time, show great promise in providing both depth and breadth of measurements for comprehensive biological information from heterogeneous cell populations. It should be noted that cellular heterogeneity can originate from clonal population, cell cycle status difference during proliferation, or environmental fluctuations significantly affecting cellular phenotypes and functions, represented by varying expression levels of proteins and genes.^[6–8] As such, single-cell analysis methods can be categorized according to the target analyte, inclusive of genomics, transcriptomics, proteomics, and metabolomics.^[9–12] Single-cell genomics and transcriptomics, e.g. such as single-cell sequencing, can be used for lineage tracing of the origins of the cellular phenotypes to understand the cell heterogeneity.^[13] Single-cell proteomics have largely permitted cellular functional analysis by identification of secreted (or secrete-able) biomolecules to elucidate cellular functional heterogeneity and intercellular communication, which is of great importance for signaling-pathway discovery, disease diagnosis and monitoring, and drug development.^[11,14–16] Here, we will mainly discuss the recent advances in single-cell secretomics, a subarea of proteomics, enabled by new microfluidics and biosensing methods.

Over the past decade, microfluidics have been extensively investigated and integrated with biosensing platforms due to their superior capabilities in fluid handling, cell manipulation, and signal amplification. Specifically, precise solution transportation enabled by the laminar flow generated in microscale channels permits controllable condition tuning of the cellular

J. He, Prof. P. Chen
Materials Research and Education Center
Materials Engineering
Department of Mechanical Engineering
276 Wilmore Laboratories
Auburn University
Auburn, AL 36849, USA

A. T. Brimmo, Prof. M. A. Qasaimeh
Division of Engineering
New York University Abu Dhabi
Abu Dhabi, UAE

A. T. Brimmo, Prof. M. A. Qasaimeh, Prof. W. Chen
Department of Mechanical and Aerospace Engineering
New York University
Brooklyn, NY 11201, USA
E-mail: wchen@nyu.edu

 The ORCID identification number(s) for the author(s) of this article can be found under <https://doi.org/10.1002/smt.201700192>.

DOI: 10.1002/smt.201700192

environment. Thus, it can be used to provide biologically relevant microenvironments for single-cell analysis with carefully managed solution physico-chemistry at high spatial and temporal resolution. Moreover, the flexible design of microfluidic structures allows the isolation of single cells of interest from a cell population, by either confining the cells in a functionalized microstructural surface (e.g., microwells), or trapping/sorting the target cells using force gradients generated by specially designed electromagnetic fields.^[17–20] In addition, the miniaturized microsystem provides a highly confined, custom environment that can significantly increase the local concentration of proteins secreted from the cells. This could potentially make protein detection more sensitive with much faster assay time, owing to the reduced diffusion distance and enhanced analyte transportation. All these unique advantages, along with the ease of fabrication, miniaturization, and integration, render microfluidics a promising platform for single-cell analysis. Here, we will firstly present the rapidly evolving microfluidic technologies, focusing on single-cell manipulation with great potential to facilitate the subsequent downstream actions.

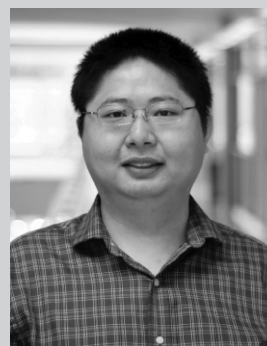
Microfluidic systems offer a powerful means for upstream sample processing in isolation, purification, concentration, and culturing of single cells of interest from a heterogeneous cell population. To meet the challenges inherent to single-cell secretomic analysis, downstream analytic techniques capable of accurate and rapid quantification of cell-secreted proteins at the single-cell level are essentially required. Given the small molecular weight and the ultralow concentration of the proteins released by individual cells, the sensitivity of the analytic tools has always been one of the critical issues that hinders the implementation of biosensing technologies for single-cell analysis. Moreover, the similar intrinsic physicochemical properties of the proteins, such as mass, size, surface charge, surface chemistry, and tertiary structure, render it even more challenging to detect target proteins in the complex biological milieu of simultaneously discharged biomolecules. To overcome these barriers, tremendous efforts have been made toward highly multiplexed and high-throughput techniques to document protein-secretion profiles. Variations of assays, e.g., bead arrays (Luminex technology), enzyme-linked immunospot (ELISpot) assay, and DNA barcode microarrays, have been developed to enable multiparametric secretomic analysis with a level of multiplexing that significantly exceeds traditional methods.^[21–23] Nonetheless, the majority of these assays requires intensive labeling procedures, and thus can only take a snapshot of the continuous secretion process. Recently, there has been an increased emphasis on the ability of capturing the protein-secretion dynamics of individual cells and the subsequent intercellular communication between neighboring cells. The addition of such temporal information to the single-cell measurements would undoubtedly enrich our understanding of the state and evolution of individual cells and their functional roles in a biological response. Thus, in the second part here, we will primarily discuss the state-of-the-art biosensing techniques that could potentially allow real-time, multiplex, and high-throughput detection of secreted proteins at a desired sensitivity and specificity for single-cell analysis. Additionally, the integration of the cell-manipulation microfluidics with adequate biosensing tools into an automated,



Mohammad A. Qasaimeh is an Assistant Professor of mechanical and biomedical engineering at New York University Abu Dhabi (NYUAD), and with the Tandon School of Engineering, New York University, Brooklyn, USA. Prior to joining NYUAD, he was a Postdoctoral Associate and Research Fellow at Massachusetts Institute of Technology and Harvard Medical School. Dr. Qasaimeh completed his Ph.D. degree in biomedical engineering at McGill University. His current research interests include developing MEMS and microfluidic devices for biological and clinical applications.



Pengyu Chen is currently an Assistant Professor in materials engineering in the Department of Mechanical Engineering at Auburn University, since 2016. He received Ph.D. in nanomaterials and biophysics from Clemson University in 2012 and worked as a research fellow in mechanical engineering at the University of Michigan for three years. His research focuses on nanoplasmonic materials, bio-nano interfaces, and biosensors for precision medicine and food safety.



Weiqiang Chen is an Assistant Professor of mechanical and aerospace engineering at New York University. He received his Ph.D. in mechanical engineering from the University of Michigan in 2014. His group is interested in developing bio-microelectromechanical systems (BioMEMS), lab-on-a-chip, biomaterials, and microsystems for studying cell mechanobiology, cancer, and stem cell biology.

robust, and user-friendly lab-on-chip device would ultimately benefit both fundamental biological research and clinical studies (see **Figure 1**). A brief discussion of the challenges and an outlook of the integrated microfluidic system for single-cell secretomic analysis toward future diagnosis and medicine is also presented.

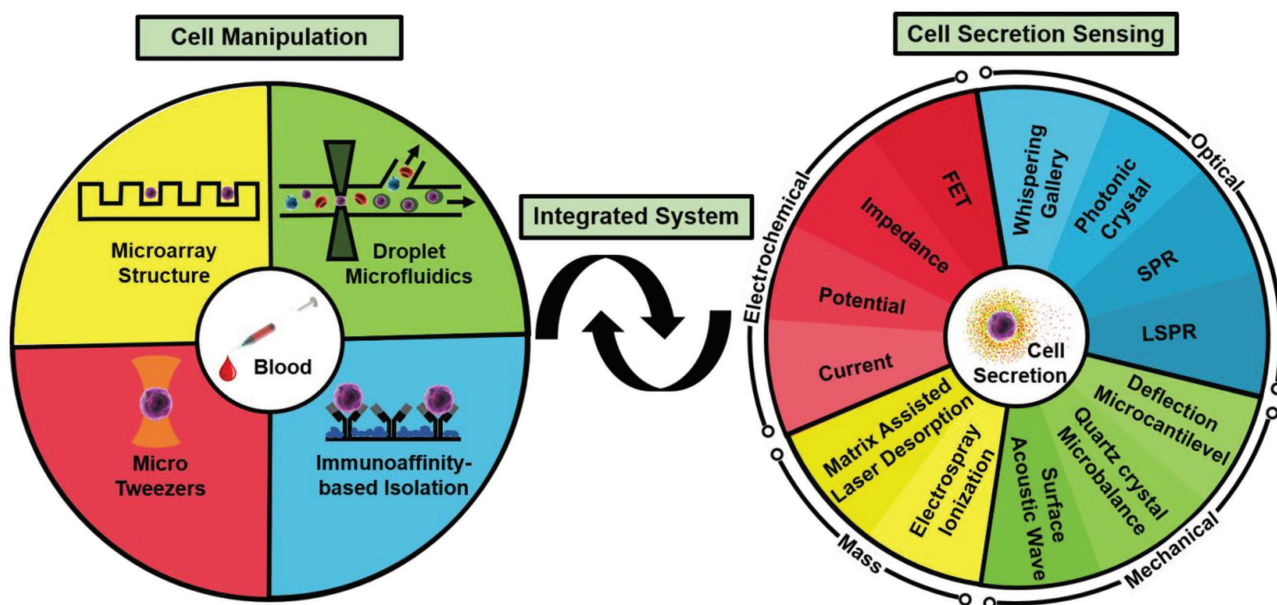


Figure 1. Concept of integrated microfluidics-based single-cell sensing system enabled by the combination of cell-manipulation and cell-secretion sensing technologies. Current single-cell manipulation methods mainly include microfluidic droplet isolation, antibody- or aptamer-based immunoaffinity purification, micro-tweezers-based manipulation, and microarray trapping, as shown in the left panel. The dynamic protein-secretion profiles from isolated single cells can be subsequently analyzed using label-free sensing technologies, including mass spectroscopy, and mechanical-, electrochemical-, and optical-based biosensing, as listed in the details in the right panel of the figure.

2. Microfluidic Systems for Single-Cell Manipulation

An ideal single-cell secretomic platform will allow the immobilization of biological cells in close proximity to the sensing region to enable continuous detection or reuse the cells for additional analysis.^[24] These processes are consequential to the sensitivity, rapidness, reproducibility, and reusability of the device. Hence, ensuring the stability, purity, and capture efficiency of single cells at defined locations is among the most important aspects of the system. As an attempt to provide guidance for optimal selection and design of a suitable capture mechanism utilizing microfluidics for single-cell analysis, this section briefly overviews the most commonly used microfluidic technologies applicable for cell sorting, isolation, and manipulation. These techniques include droplet encapsulation, flow cytometry (fluorescence-activated cell sorting), antibody-assisted capturing, micro-array-isolation, and field-gradient-based tweezers (such as optical, electrical, magnetic, acoustic, and hydrodynamic tweezers).^[25–28]

2.1. Droplet Microfluidics for Single-Cell Sorting and Analysis

Microfluidic droplet-isolation techniques encompass the use of droplets to encapsulate biomolecules, single particles or cells in a confined microenvironment. This method offers a high-throughput approach to isolate target species using only a picoliter sample volume. Since the molecules released by the encapsulated single cells are confined and enriched in a droplet, this technique overcomes a major challenge in single-phase microfluidic systems due to analyte dispersion, and has

been widely exploited as a molecular concentrator for secreted molecules.^[29–37] Other advantages of the droplet-isolation technique include the ability to: i) precisely tune droplet sizes to control the microenvironment; ii) encapsulate single cells with other reagents to mimic physiologically relevant conditions; and iii) manipulate droplets for sorting, purification, and other downstream analysis.^[38–42]

The classical way of generating droplets is via break-up at a T-junction – shearing a liquid into another immiscible one, often in the presence of a surfactant.^[37,43,44] In microfluidics, a derivative of this technique, called the flow-focusing method, is typically adapted to encapsulate single cells.^[29,45–47] The flow-focusing setup constitutes the intersection of a carrier fluid (oil) with a cell-medium flow at a focusing geometry, and integrated into planar microchannels in the form of a cross junction (see **Figure 2a**).^[45] This co-flow with carrier oil produces “water-in-oil” emulsion droplets that can encapsulate any cell, particle, or molecule present in the cell-culture medium. Perfluorocarbon oils have been commonly used as the carrier fluid, since they are compatible with poly(dimethylsiloxane) (PDMS) devices, immiscible with water, and relatively transparent to allow optical detection and readout procedures.^[29] By carefully controlling flow rates in both channels, single cells can be isolated within a droplet formed at intervals in a continuous oil phase. The number of cells encapsulated in each drop was found to exhibit a Poisson distribution depending on the cell-medium flow rate and cell concentration.^[45] In order to obtain reasonably pure populations of “positive” droplets with only single cells captured, the production of droplet-encapsulated cells can be coupled with additional detection and sorting processes.^[43] For instance, Brouzes et al. developed a microfluidic chip for screening single mammalian cells

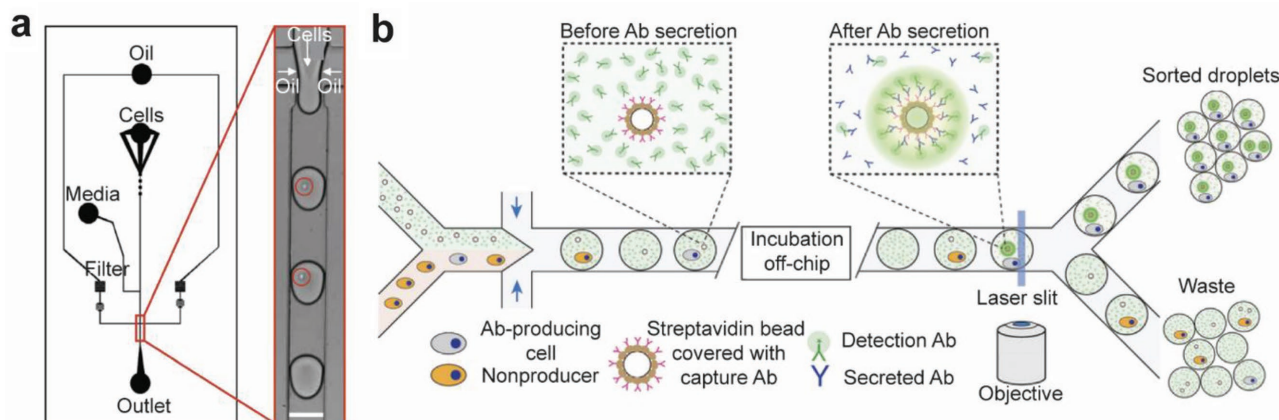


Figure 2. Microdroplet encapsulation and fluorescence sorting of single cells. a) Schematic of a microfluidic flow-focusing design for single-cell droplet encapsulation. Inset: image of the encapsulation of single cells (red circles) in picoliter droplets. Reproduced with permission.^[45] Copyright 2008, Elsevier. b) Illustration of droplet-based single-cell sorting technique. Individual cells were encapsulated in droplets with goat anti-mouse-Fc capture antibodies and free fluorescently labeled goat detection antibody. After incubation, cell-secreted antibody was captured, generating a detectable fluorescent signal. Reproduced with permission.^[50] Copyright 2013, Nature Publishing Group.

encapsulated in droplets based on cytotoxicity.^[30] Their device combined 5 serial droplet modules for a sensitive detection of live and dead cells. In another study, Baret et al demonstrated the sensing of droplet-encapsulated cells based on enzymatic activity.^[48] Fallah-Araghi et al. also used droplet-encapsulated single genes to demonstrate an on-chip DNA amplification and screening system based on the coupled transcription and translation of genes.^[49]

In addition, Charbert and Vivoy successfully developed a microfluidic system that accommodates high-throughput encapsulation of single cells into picoliter droplets, and subsequent “self-sorting” of these individual droplets purely based on hydrodynamic effects, thereby improving single-cell capture efficiency.^[30,43,46,47,51] Their system entirely relies on passive hydrodynamic effects, known as Rayleigh–Plateau instabilities in a jet flow, followed by shear-induced drift and excluded-volume-driven dispersion of individual droplets – for encapsulation and sorting. Since the drift velocity has a strong correlation with the droplet diameter, single-cell-encapsulating droplets, which typically possess larger diameter than that of empty ones, can reach the center of the focusing channels more rapidly, leaving others remaining on the stream line. This size-/time-based discrepancy can be used to initiate the “self-sorting” of cell-containing droplets in the focusing region. Even if numerous cells flow in close vicinity to the focusing area, they are hydrodynamically separated from each other and individually aligned to prevent encapsulation of multiple cells in a single droplet.^[43,52] This hydrodynamic droplet-based encapsulation and sorting method is well suited for applying single-cell molecular analysis, such as PCR and enzymatic assays.

Fluorescence-activated cell sorting (FACS) is a technique that can distinguish cells of interest on their light-emitting properties. This system has been widely used to identify and sort individual target cells either by direct fluorescent labeling of fixed cells or by specific fluorescently labeled antibodies attached to the cells (see Figure 2b).^[53,54,50] As described in the previous section, cell-encapsulating droplets act as a diffusional barrier between the cells and the surrounding medium

to enable reactions of the locally confined molecules in the droplet.^[55] Thus, instead of direct sorting of cells in the flow medium, droplet-based FACS enables on-chip assay and cell selection according to changes in the local extracellular media in the droplet, induced by cell-specific processes.^[44] Originally devised using Fulwyler’s cell-sorting unit and Sweet’s droplet-deflection methods, this technique generates a stream of cell-entrapping droplets and electrostatically deflect these droplets containing stained cells.^[56,57] Early use of this device for single-cell isolation include the work by Liesegang et al., where one specific variety of myeloma cells were treated with fluorescently labeled antibodies and selectively sorted using the droplet FACS.^[58] A similar system was used to measure *Escherichia coli* β -galactosidase gene (*lacZ*) activity in large numbers of individual viable eukaryotic cells.^[59] Viable single cells were isolated based on their level of *lacZ* expression with a reduction of false positives using two-color measurements. More recently, FACS systems based on multicolor droplets were demonstrated that provide remarkable opportunities for high-throughput, multiplex single-cell sorting and on-chip multi-parametric cell-secretion analysis.^[50,60,61]

2.2. Immunoaffinity Purification of Cells using Antibody-Functionalized Microfluidic Chips

Given to antigen expression on a target cell’s surface, it is possible to isolate cells of interest from the cell population by employing a specific binding between the antibody and the cell-surface antigen, which enables high capturing specificity and isolation purity.^[62,63] So far, current positive single-cell-capturing technologies mostly rely on the specific binding between antibodies immobilized on the microstructure surface and surface biomarkers.^[64–66]

Carter’s observation of the isolation of cell fibroblasts on palladium (Pd) islands created on an acetate film was one of the earliest studies on cell-adhesive surfaces.^[67,68] This study pioneered cell-adhesive metallic materials, and has been now

been expanded to other materials, predominantly in polymers and self-assembled monolayers.^[69,70] However, a noteworthy aspect of the advances in cell–substrate capture technologies is the capture of circulating tumor cells (CTCs).^[71] CTCs are extremely rare, with a frequency of typically 1–10 CTCs among 6×10^6 leukocytes, 2×10^8 platelets, and 4×10^9 erythrocytes per mL of blood.^[72,73] Such a low concentration creates great technical challenges in capturing and detecting the CTCs. The ability to accurately identify, isolate, and analyze these CTCs offers immense value in fundamental and clinical cancer research, and has hence spurred numerous research activities in this area.^[74,75] The anti-epithelial-cell-adhesion-molecule (EpCAM) antigen has been recognized as the primary target molecule associated with CTCs, and has thereby been widely used in many technologies developed for CTC capture.^[73] Some noteworthy studies include the development of a unique microfluidic “CTC-chip” by Nagrath et al. that allows selective capture of viable individual CTCs from peripheral whole blood samples using antibody (EpCAM)-coated micro posts in a microfluidic chip (see **Figure 3a**).^[76] Nagrath’s group later

developed an approach for sensitive capture of CTCs by using anti-EpCAM-antibody-modified graphene oxide nanosheets on a patterned gold surface.^[77] Apart from the isolation of CTCs, isolation methodologies have also been explored based on the capture of leukocytes using an antibody target to the leukocyte surface marker CD45.^[78] Despite advantages of the antibody-based isolation, releasing captured cells is often difficult due to the strong covalent bonding between the antibody and the cell-surface receptor, posing challenges for subsequent analysis. An alternative solution is to use aptamers as a substitute of traditional antibodies because DNA-based aptamers have similar functions to antibodies yet have more advantages for biological applications.^[79] With similar specific binding characteristics to antibodies, some researchers have been reported applying aptamers on CTC isolation.^[80,81] A noteworthy consideration in capturing CTCs is that only cells with EpCAM expression can be successfully isolated using the immunoaffinity-based single-cell capture technique.^[82–84]

2.3. Microarrays for Single-Cell Trapping

Physical confinement trapping using microarray structures provides an alternative method for single-cell isolation. One of the most commonly used approaches simply relies upon the gravitational sedimentation of the cells into a microwell array for single-cell isolation, as reported previously (**Figure 3b**).^[86–91] The single-cell capture efficiency of this technique can be optimized by carefully controlling the microwell diameter, microwell depth, and the settling time.^[18,92,93] Rettig and Folch found that the total number of trapped single cells increases with the microwell’s depth but reduces with microwell width. Wider microwells can accommodate multiple cells, but the cells also tend to be more easily dislodged from the bottom of the microwells during the rinsing step.^[92] Inasmuch as most microwell applications follow the same fundamental principle, various configurations of the system are available.^[17,92] For example, for real-time monitoring of β -galactosidase expressions in living *Escherichia coli* cells, Cai et al. developed a microfluidic system that can isolate single cells in microwell arrays, with volume capacities of 100 pL, by actuating two adjacent valves in a control layer.^[17] Eyer et al. also incorporated a pneumatically controlled shutter to control the opening and closing of a microchamber array to study the intracellular biomolecules secreted from captured cells.^[18]

Recently, Son et al. demonstrated the use of microsized compartments to confine single human CD4+ T cells with antibody-functionalized streptavidin-coated microbeads.^[85] Their microfluidic device

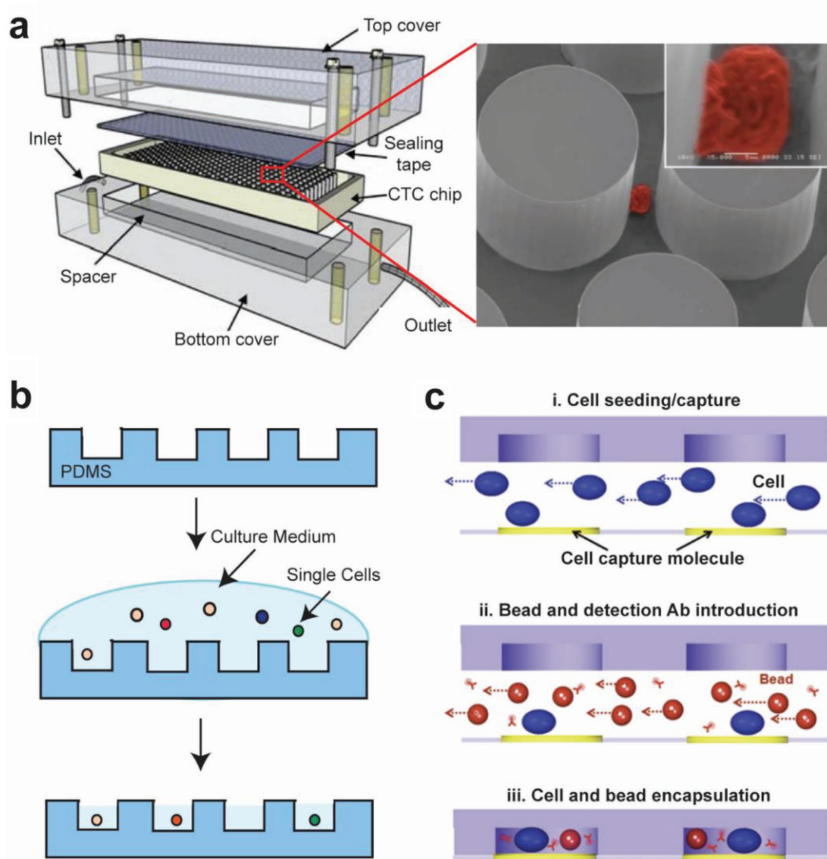


Figure 3. Micro-chamber single-cell isolation techniques. a) Left: Schematic of a “CTC chip”. Right: SEM images of spiked NCI-H1650 lung cancer cell in blood captured by the EpCAM-coated micro posts. Reproduced with permission.^[76] Copyright 2007, Nature Publishing Group. b) Illustration of using microchambers for on-chip single-cell isolation culturing and incubation. c) Schematics of cells/sensing beads encapsulated inside a microarray compartment. Individual compartment consisting of single cells and sensing beads allows in situ protein-secretion detection. Reproduced with permission.^[85] Copyright 2016, The Royal Society of Chemistry.

consisted of a microchamber array with a reconfigurable top layer and an antibody-patterned cell-adhesive substrate. This set-up incorporated both the surface-function and the passive-confinement methods to capture individual cells first and confine them in the microwell to monitor the interferon gamma (IFN- γ) secretory activities using a bead-based sandwich immunoassay (Figure 3c). In a separate study, the same group used a micropatterned photodegradable hydrogel array integrated with the reconfigurable microwell array that enabled on-chip single-cell trapping and retrieval.^[94] Other notable single-cell applications using microarray structures include hematopoietic stem cell (HSC) proliferation control, HSC self-renewal monitoring, and microscale tissue engineering.^[95–97] All these studies show the microarray system as a powerful tool for single-cell manipulation with unique advantages in simplicity, low-expertise requirements, ease of fabrication, and high compatibility with a wide range of sensing methodologies for subsequent analysis.

2.4. Microparticle Tweezers

The mechanism of micromanipulation of single cells characteristically constitutes the generation of a field gradient strong enough to confine and then manipulate the cells. These micromanipulation devices are commonly known as microparticle tweezers based on optical, electrical, magnetic, acoustic, and hydrodynamic field gradients.^[27,28]

Optical tweezers use radiation-pressure forces from a focused laser beam to trap micrometer-sized neutral particles.^[19,98–101] These devices can isolate objects as small as 50 nm, with forces exceeding 100 pN and temporal resolutions as fine as 10^{-4} s.^[102,103] Soon after its first use as an atom trap in 1969, the technique was used to trap and manipulate living cells.^[104,105] Isolation of viruses with a power of about 100 mW was easily achieved, but optical damage of bacteria at this power level was apparent.^[105] However, using a 1.06 μm neodymium-doped yttrium aluminum garnet (Nd:YAG) laser, significant decrease in damage to bacteria was observed, which led to further applications of the optical trap in measuring the elastic properties of cytoplasm.^[106,107] The aforementioned studies pioneered the field of damage-free optical trapping of bioparticles and influenced several monumental studies that applied this trapping technology to isolate and manipulate bacteria flagella, chromosomes during cell division, live sperm cells, molecular motors, RNA polymerase enzyme, and bacteria in high-temperature environments.^[108–111] In microfluidics, fundamental work by Wang et al. on measuring escape velocity, trapping efficiency, and fluorescent intensity for micrometer-sized spheres was one of the first to apply optical tweezers.^[112] Following this, a wide range of studies focused on using optical tweezers for non-invasive and high-precision sensing and/or sorting of microparticles in microfluidic systems.^[20,113–118] The use of optical tweezers for stretching single red blood cells and DNA molecules has also been demonstrated.^[119,120] It is important to know that, although the term “cell sorting” does not necessarily mean single-cell isolation, some of these cell-sorting devices offer single-cell isolation. Another quite interesting application in microfluidics is the quick (less than 0.2 s) and reversible change of medium around a cell.^[121,122] More-comprehensive reviews of optical tweezers can be found in the references.^[28,100,102,123]

Magnetic tweezers operate by inducing stagnation forces through a magnetic field gradient. The method is noninvasive, allows micromanipulation without direct contact, has a spatial resolution that ranges between 2 nm and 10 nm, and applies forces ranging between 0.01 and 10^{-4} pN.^[103] These systems have numerous designs with a varying level of complexity, and typically entail a configuration of permanent magnets or electromagnets mounted on the stage of an optical microscope.^[124] In biological applications, two types of cells are naturally magnetic: red blood cells because of their paramagnetic hemoglobin, and magnetotactic bacteria that synthesize intracellular chains of magnetic nanoparticles, and hence can be directly manipulated using magnets.^[125,126] To use magnetic tweezers for all other type of cells, magnetic labeling – internally or externally attaching magnetic beads – is required.^[127] The fascinating applications of magnetic tweezers include manipulation of cancer cells, single molecules, cell surfaces, and filamentous macromolecular networks, and intercellular manipulation.^[128–138] Biosensing applications of magnetic tweezers include giant-magneto-resistive (GMR) sensors, spin-valve sensors, miniaturized Hall sensors, and superconducting quantum interference devices (SQUIDs).^[139–145] Recently, Chang et al. reported an application of a 3D microchannel electroporation (MEP)–magnetic tweezers (MT) integrated chip to deliver the GATA2 molecular beacon into leukemia cells to detect the GATA2 gene’s regulation level associated with the initiation of leukemia.^[146]

The most predominantly applied electrical particle-manipulation mechanism in microfluidics is dielectrophoresis (DEP) – the motion of electrically polarized particles relative to that of their solvent.^[147] Although, Pohl’s investigation on removing suspended solid particles from polymer solutions using this concept is widely cited as the first to describe the phenomenon, Henry’s 1924 patent of this concept predates any other application.^[27] Based on the original design, depending on the system’s configuration, a trapped particle can be made to move either toward the high field gradient (p-DEP) while experiencing a positive dielectrophoretic force, or toward the low field gradient (n-DEP) while experiencing a negative dielectrophoretic force. However, over the years, several configurations have been devised to facilitate trapping with simultaneous p-DEP and n-DEP quadrupoles (2D), in 2D arrays, with 3D electrodes, and in sub-micrometer resolution.^[148–152] Biomedicine has been the most influential driver of DEP applications; with a relatively high volume of such research focused on cells, bacteria, DNA, and viruses.^[147,153–165] Other bioparticles that have been successfully manipulated using this technique include stem cells, neurons, apoptosis, chromosomes, and proteins.^[166–170] In addition, substantial progress has been made toward translating the theoretical treatment of bioparticles to practical applications as biosensors and other integrated functions like electroporation and microinjection with a single probe.^[150,171] One of these applications includes that of Park et al., where the development and proof-of-concept of an integrated microfluidic biochip, with DEP tweezers and sensing electrodes applying the impedance-detection method, was demonstrated for single-cell applications.^[172] The proposed microfluidic chip consists of trapping chambers equipped with the sensing and actuation electrodes for single-cell monitoring and DEP applications respectively

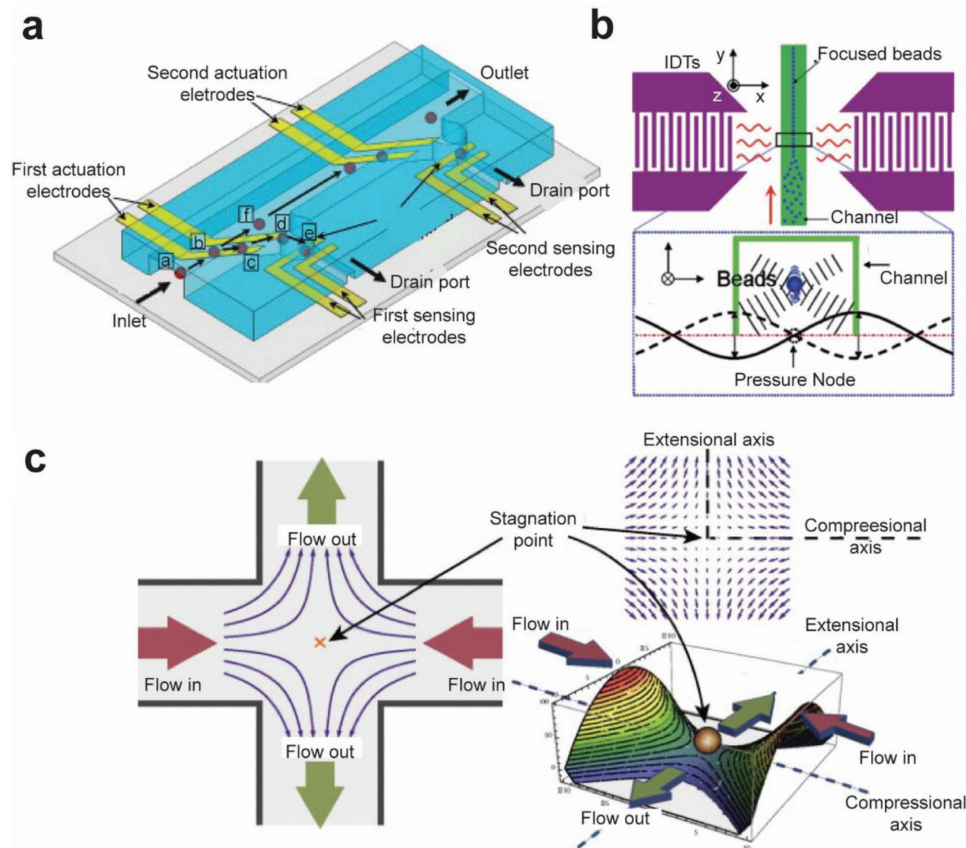


Figure 4. Applications of the single-cell tweezers. a) The typical setup for DEP actuation and subsequent impedance chip. Reproduced with permission.^[172] Copyright 2010, Elsevier. b) Schematic description of the working principle of the SSAW focusing device. Inset: illustration of the SSAW pressure field inside the channel with beads focused at the pressure node. Reproduced with permission.^[173] Copyright 2008, The Royal Society of Chemistry. c) Hydrodynamic trap created by a planar extensional flow field at the junction of two perpendicular microchannels. The right panel shows the velocity field (top) and the potential well (bottom) exerted on a particle in the flow field at the microchannel junction. Reproduced with permission.^[174] Copyright 2010, AIP Publishing LLC.

(see **Figure 4a**). Cells at the actuation electrodes are forced into the trapping chamber by negative DEP to create an impedance increase between the sensing electrodes – due to the cell's blockage of the electrical conducting path between the two sensing electrodes. This impedance shift is hence used to electrically monitor cell trapping, which acts as a sensor for dynamically controlling the DEP signal on the actuation electrodes – when a cell is captured by the first chamber, the DEP is turned off and subsequent cells pass the first trapping chamber to be captured in the next chambers using the same mechanism.

In acoustic tweezers, stationary pressure gradients generated from a standing ultrasonic wave are used to exert forces on particles in a medium that are discernible by density and compressibility (see **Figure 4b**).^[173] The theories behind acoustic pressure have been long developed and generalized.^[175] While investigating the effects of low-intensity ultrasound on blood circulation in living tissues, Dyson et al.^[176] observed an aggregation of red blood cells, and Baker^[177] suggested that this behavior is primarily caused by the standing wave. These studies pioneered the field of acoustic traps and later influenced studies aimed at manipulating cells using ultrasonic standing waves.^[178,179] During the early days, the viability of trapped cells was a topic of discussion, but more recently, the technique has been

demonstrated to be practical for viably trapping cells and yeast during culture experiments.^[180,181] In a similar fashion, Neild et al. built an acoustic sorting device that can produce 2D arrays of cells, which has a potential application in drug screening and sequential cell treatment.^[182] Another noteworthy advancement of the acoustic trap is the development of focused ultrasonic waves to enhance sensitivity of bead-based bioaffinity assays, their use in enriching cells from dilute samples or rare-event experiments, use as continuous flow microfluidic sorters, for patterning cells, and its integration as a major component of a single-layer microfluidic chip.^[68,183–188]

The majority of purely hydrodynamic tweezers make use of the stagnation point generated by extensional flows – adjacent layers of flow toward or away from each other – to manipulate particles (see **Figure 4c**).^[174] The first use of these types of stagnation flows can be traced back to 1930, where they were generated using four-roll mills to investigate the deformation and burst of droplets in an emulsion.^[189] During the early stages of its adoption, a major issue was the instability of the generated stagnation point, which was solved by the feedback control system originally developed by Bentley and Leal.^[190–192] Following these, studies in microfluidics adapted a “cross-slot” apparatus – named for the resemblance to the four arms of a cross, with flows injected

via two opposite channels and concurrently sucked out via the other two channels – to generate stagnation flows.^[193] Although predominantly used to study polymer-droplet dynamics, the cross-slot has been adapted for some biological applications like DNA stretching/compaction, quantitative assessment of cell mechanical damage, and for detecting DNA target sequences and marker position.^[194–198] More recently, stagnation flows have been developed with open microfluidic systems in the form of microfluidic pipettes and probes, to collect vesicles and perform cell analysis respectively.^[199–205] The microfluidic probe has been further developed to generate the microfluidic quadrupole trapping mechanism, which has been used to study neutrophil chemotaxis.^[206,207] Detailed reviews on the application of microfluidic quadrupoles can be found in ref. [208].

2.5. Other Mechanisms

In microfluidic channels, there are several other particle-sorting mechanisms that exploit discrepancies in the physical features of particles to facilitate separation. Inertial forces have been used to reduce the focusing of randomly distributed particles and CTCs, to a single point within a channel, for high-throughput separations. This occurs due to the superposition of the shear-induced lift force and the wall-induced lift force. This type of sorting has been reported by Di Carlo et al.^[209] and Ozkumur et al.^[210] The influence of centrifugal acceleration on inertial forces has also been exploited to sort CTCs based on the formation of two symmetrical counter-rotating vortices across a microfluidic channel.^[211] This technique is called Dean flow fractionation (DFF), after the pioneering work on such vortices in curved pipes.^[212] A comprehensive review of centrifugation forces for cell separation can be found in ref. [213]. Hydrodynamic filtration is another size-based separation technique in microfluidics.^[214] A configuration of this technique involves passing flow through a channel with multiple suction-flow side-branching channels. The side-channel suction flows align the particles along the main channel's wall with smaller-sized particles closer to the wall, hence being suctioned earlier. The use of cross flow filters – which allow cells smaller than the membrane pore size to pass while separating larger-sized cells – has also been reported.^[215] Another technique is based on positioning sieves along the centerline of the flow channel for sequential isolation. In this configuration, the first cell is trapped in the first sieve, and the second cell bypasses the first sieve to be trapped by the second sieve positioned with an offset from the first sieve.^[216] It is important to note that while some of these examples are not explicit single-cell biosensing applications, the bounding principles are very much applicable. In-depth reviews of some of these techniques can be found in refs. [27] and [217].

3. Biosensors for Label-Free Detection of Single-Cell Protein Secretion

Microfluidics-based on-chip single-cell isolation/manipulation techniques enable effective upstream cell-sample preparation, which overcomes the two extreme challenging tasks in high-efficiency cell enrichment and precise single-cell capture.

Combined with recent advances in microfluidic large-scale integration (mLSI), miniaturized device dimensions, controllable microenvironments, and highly parallel measurements in single chips can be realized. Microfluidics thereby offers unprecedented opportunities to individually analyze the target of interest using a series of analytical tools.^[22,218–220] Single-cell analysis can be a very broad topic that spans across a wide range of analyte molecules produced by cells, including proteins, hormones, enzymes, metabolites, microRNA, and reactive oxygen species (ROS), which play key roles in cell differentiation, proliferation, communication, and migration. Thus, being able to detect these secreted molecules at single-cell resolution clearly provides great insight in cell phenotype or function and their connections to physiological or pathophysiological processes.

Conventional methods such as flow cytometry and ELISpot are regarded as the gold standards for single-cell analysis (see Figure 5a).^[221–223] However, these approaches typically involve complex functionalization, immobilization, incubation, and washing steps, with a long assay time. Hence, they are limited to static measurements and do not completely satisfy the increasing demand of adding dynamic information in single-cell analysis. In this section, we focus our discussion on a subarea of single-cell analysis, namely single-cell secretomics using label-free biosensors. We particularly describe biosensing methodologies for label-free protein detection and the advantages and potential limitations of these technologies to enable kinetic measurements of the ordering and timing of protein secretion by single cells.

3.1. Mass Spectrometry for Protein Detection

Mass spectrometry (MS) is a sensitive, high-throughput and label-free analytic technique that detects ionized analytes based on their mass-to-charge ratio. MS was limited to the detection of small molecules for a long time, as there were no effective techniques available to noninvasively ionize the samples without excessive structure damage.^[227] This barrier was breached by the development of matrix-assisted laser desorption/ionization (MALDI). Upon laser irradiation, the matrix compounds absorb most of the energy, which minimizes the destruction of the ionized analyte. So far, applications of MALDI-based mass spectrometry are predominantly in proteomics, metabolites analysis, and protein quantification.^[224,228–232] A representative example for the detection of cell-released metabolite was demonstrated by Amantonico et al., as shown in Figure 5b.^[224] However, the complicated and bulky instrument requirements for ionization and detection greatly hinder the application of MS for single-cell secretomics. Until recently, Yang et al. developed a MALDI-mass-spectrometry-based immunoassay by integrating the MS system in a microfluidic platform, which allows the detection of insulin secretion at the single-cell level.^[233] A detection limit of 50 nM was achieved by the MS spectrum at a signal-noise ratio of 4.3. Later, this system was further miniaturized by using an on-chip pulse-heating ionization, as demonstrated by Sugiyama et al.^[234] Using this approach, protein ionization was realized by the thermal energy provided by a Pt/Cr microheater, coupled with a time-of-flight (TOF) filter for detection. Although these

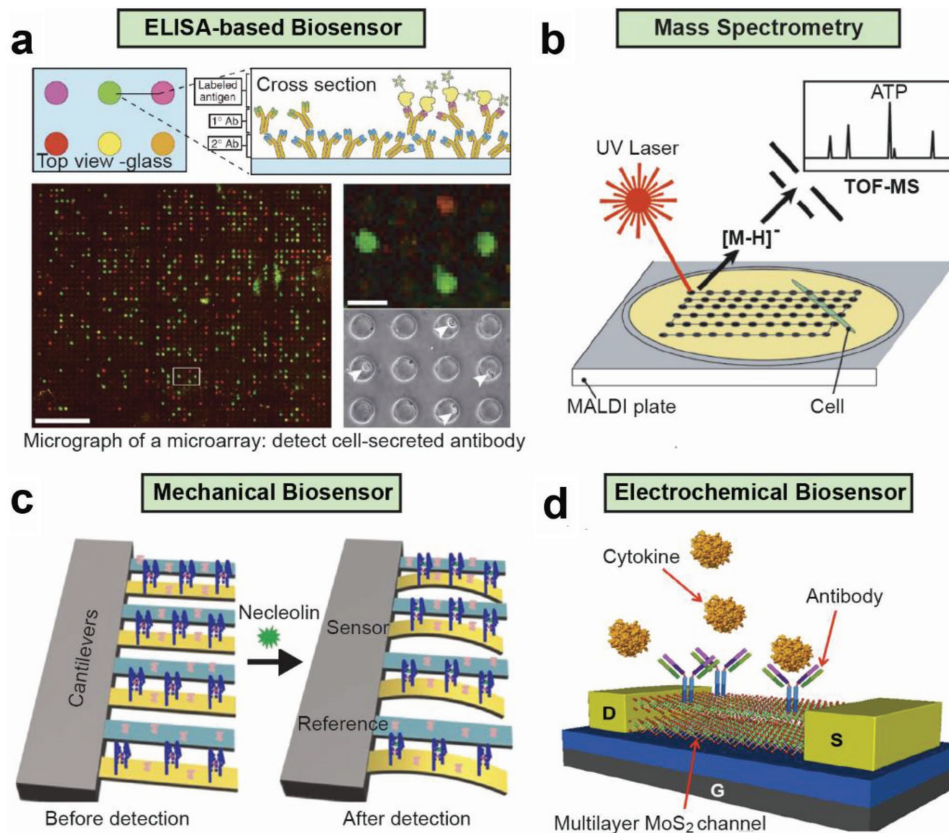


Figure 5. Standard ELISA method and label-free biosensors applied in single-cell protein sensing. a) Cell-secreted antibodies were captured by secondary antibodies immobilized on glass surface. The complex formation of fluorescently labeled antigen–secondary-antibody–primary-antibody produces a detectable signal. Reproduced with permission.^[223] Copyright 2006, Nature Publishing Group. b) Single cells encapsulated in droplets were deposited on a MALDI plate. The metabolites produced by single cells were extracted by 5'-monophosphate, and co-crystallized with the MALDI matrix, followed by MS analysis. Reproduced with permission.^[224] Copyright 2010, American Chemical Society. c) A schematic illustration of the nucleolin microcantilever-based biosensor. Sensing microcantilevers (blue) were functionalized with nucleolin aptamer and blocked with MCH, while reference microcantilevers (yellow) were only blocked with MCH. The induced displacements of the sensing microcantilevers by aptamer–nucleolin specific binding were detected. Reproduced with permission.^[225] Copyright 2016, Elsevier. d) A multilayer-MoS₂-based FET biosensor was used for the detection of TNF- α . Reproduced with permission.^[226] Copyright 2015, American Chemical Society.

inexpensive, integrated MS-based biosensing platforms offer unique capabilities of sensitive, high-throughput determination of protein secretion from single cells, such measurements still require an assay time of around 4 h, and thus fall in short in providing the dynamic secretion information in a fine time resolution. Moreover, accurate identification and quantification of the secreted proteins remains a big challenge, especially when measuring complex biological samples. In situ detection of proteins produced by isolated cells in a confined microenvironment need extra efforts to avoid potential damage to the cells by sample ionization.

3.2. Mechanical Protein Biosensors

Mechanical biosensing is a rapid, label-free detection method that measures the surface deflection or resonance shift resulting from surface stress or mass change upon analyte–receptor interaction. Binding of the analyte can be quickly detected and transduced into the signal response of a bending

or vibration frequency change, which has facilitated the employment of mechanical biosensors for real-time detection of biomolecules, bacteria, and cells.^[235–237] In the following sections, we present three major mechanical protein biosensors based on their sensing modalities including, microcantilever deflection, quartz-crystal microbalances, and surface acoustic waves.

3.2.1. Microcantilever-Deflection-Based Protein Detection

Microcantilevers are microscale structures that can act as a physical, chemical, or biological sensors by detecting changes of the cantilever deflection induced by weight variations on their surface. The advancement of microelectromechanical system (MEMS) technology allows the development of parallel, microfabricated cantilevers for on-chip measurements with increased experimental throughput. Li et al. reported a deflection-based mechanical-sensing platform using a microcantilever array for the detection of nucleolin (see Figure 5c).^[225] The microcantilever array was

composed of eight silicon cantilevers ($500\ \mu\text{m} \times 100\ \mu\text{m}$), with a 3 nm titanium layer, and a 20 nm gold layer. The interaction between microcantilevers functionalized with nucleolin and nucleolin aptamer (AS1411) resulted in a differential deflection between the reference cantilevers and the sensing cantilevers, which was measured by a commercial optical-beam deflection system. This system required a short assay time of only about 12 min, suggesting its potential for real-time protein detection. The cantilever array enabled parallel measurements with reference microcantilevers, improving the statistic accuracy and reducing system error. However, this technique suffered from relatively low sensitivity (only 1 nM) when measuring small proteins because of the intrinsically small surface-stress variation upon binding. Introduction of secondary recognition elements labeled with particles of large mass can allow potential use for signal amplification.^[238] However, this inevitably increases the total assay time and compromises the capability of accessing real-time information. By incorporating a piezoelectric material ($\text{Pb}(\text{Zr}_{0.52}\text{Ti}_{0.48})\text{O}_3$) layer on the microcantilever, Lee et al. demonstrated a mechanical-resonance-frequency-based antigen-detection method with a detection limit down to $10\ \text{pg mL}^{-1}$.^[239] However, this technique only offers static measurements with end-point readout, thus needing further improvements to allow real-time single-cell secretion analysis.

3.2.2. Quartz Crystal in Microbalance-Based Protein Detection

The quartz crystal, as a highly precise and stable oscillator, has attracted much attention for biosensing applications. The underlying mechanism of the quartz-crystal microbalance (QCM) for protein detection is based on the oscillation-frequency variation caused by the mass change, as expressed by the following equation:

$$\Delta F_n = -N \frac{2F_0^2}{A\sqrt{\mu\rho}} \Delta m \quad (1)$$

where ΔF_N is the change of oscillation frequency, N is the order of overtone, F_0 is the fundamental frequency, A is the electrode area, μ is the shear modulus, ρ is density of the quartz crystal, and Δm is the mass change.^[240] The application of the QCM as a biosensor was first demonstrated by Sota et al. in the detection of myoglobin.^[241] Briefly, a rectangular quartz-crystal resonator was fixed on a solid support with an extremely thin gold layer on top serving as electrodes and leads. These electrodes provided an alternative electric field, leading to the quartz crystal vibrating at its resonance frequency. The capture of the analyte on the functionalized quartz-crystal resonator reduces the oscillatory frequency and has thus been employed as a convenient, label-free method for biomolecule quantification. However, this technology's low sensitivity ($\approx\text{nM}$) and relatively complex sensing scheme have limited its exploitation for single-cell secretomics.^[235,242]

3.2.3. Detection based on Surface Acoustic Waves

The surface acoustic wave (SAW) represents another promising real-time and label-free mechanical-sensing technique.

By applying a propagating acoustic wave on the surface of a piezoelectric crystal, the mass change of the crystal leads to the frequency variation of the applied wave. A representative example for SAW biosensors was demonstrated by Lee et al. for the detection of hepatitis B surface antibody.^[237] Shear horizontal waves were introduced by an input interdigitated transducer (IDT), and were trapped near the crystal surface by a guiding layer. The hepatitis B surface antibodies in a sample of blood were captured by hepatitis B surface antigens immobilized on the crystal surface. The resulting acoustic-wave frequency change was monitored by an output IDT. This platform enabled the real-time detection of antibody-antigen binding with an impressive detection limit of $10\ \text{pg mL}^{-1}$. The same group later utilized a signal-amplification method by the aid of gold nanoparticles to further improve the sensitivity.^[243] The potential drawbacks of this device for integrated single-cell analysis systems could be the lack of multiplex capability and potential difficulty in sensor miniaturization and integration.

3.3. Electrochemical Biosensors

Binding of target proteins can also be detected by converting the electrochemical activities inherent in analyte-antibody interactions to electrical signals, such as current, potential, and impedance.^[244–252] Sensing techniques based on this principle is known as electrochemical biosensing. Compared to the mechanical biosensors, electrochemical methods that typically exhibit higher sensitivity do show certain advantages in single-cell protein sensing. However, they also face some challenges, particularly when dealing with real biological samples with high ion strength and diverse interfering molecules. The following sections discuss the various types of electrochemical biosensors.

3.3.1. Current-Based Electrochemical Detection

Conventional amperometric biosensors measure the variation of the current in redox reactions that are associated with immunoreactions.^[246,248] Owing to its simplicity, low cost, and ease of miniaturization, this method has been applied in protein detection, exosomes, microRNA, and virus recognition.^[250,253–257] However, the redox reaction usually requires an electron-transfer reagent, limiting its usage for recording the dynamic information in a biological reaction. Only a few attempts have been made to employ this technique for real-time biomolecule detection. Hsieh et al. reported a microfluidic electrochemical quantitative loop-mediated isothermal amplification (MEQ-LAMP) system for real-time measurement of pathogenic DNA.^[258] Another amperometric biosensor was demonstrated by Liu et al. for label-free detection of IFN- γ .^[253] As opposed to the traditional method to detect the signal from the enzyme catalytic redox reaction, this sensor utilized the current variation caused by changes of aptamer conformation upon target binding. Specifically, one end of the IFN- γ -specific aptamer was immobilized on a gold electrode, while the other end was functionalized with Methylene Blue (MB) molecules. The aptamer was designed to form a hairpin structure, which brought the MB molecules close to the gold surface, resulting in a high

current due to electron transfer from the MB to the electrode. Upon sample loading, the binding of IFN- γ unraveled the hairpin loop, sending the MB redox molecules away from the gold electrode, thereby generating a decreased current. A detection limit of 0.06 nM of IFN- γ detection was achieved. Based on this approach, a few studies have been carried out by the same group to monitor the dynamic cytokine secretion from isolated immune-cell populations and the molecular signaling in intracellular communication, showing it a promising platform for single-cell protein analysis.^[259,260] The major constraints of this technology are the limited availability of verified aptamer sequences and the relatively low binding affinity of aptamers compared to antibody-based capturing mechanisms.

3.3.2. Field-Effect-Transistor-Based Protein Detection

Recent advances in 2D nanomaterials have drawn great attention and created vast opportunities for field-effect-transistor (FET)-based biosensors. FET is very sensitive to changes in local electric properties induced by small variations on the material surface. Hence, various 2D nanomaterials with superior electric properties, such as: silicon nanowires, carbon nanotubes, metal oxides, and organic semiconductors, have been integrated into FET protein sensors.^[261–266] For example, Pui et al. demonstrated a silicon-nanowire FET biosensor for real-time measurement of tumor necrosis factor-alpha (TNF- α) and interleukin-6 (IL-6) secreted from macrophages.^[267] Two n-type field-effect-dominant silicon nanowires were functionalized with different antibodies in separated sensing regions. Due to the difference in the isoelectric points between the TNF- α (5.08) and IL-6 (6.91) and the opposite surface charges of these two cytokines at pH = 6, the binding of TNF- α and IL-6 onto the silicon nanowires yielded completely different responses in conductance. This platform offers ultrasensitive (\approx 100 fM) cytokine detection using only 20 nL of the sample with a potential to be expanded for multiplexed single-cell protein measurement. A similar but more sensitive FET biosensor that employed the multilayer MoS₂ structure for the detection of TNF- α was reported by Chen et al., as shown in Figure 5d.^[226] Recently, electrolyte-gated organic field-effect transistors (EGOFETs) have gained increasing interest due to their low cost, biocompatibility, and ease of fabrication.^[268–270] More importantly, the low-gate-potential requirement offered by the large capacitance of the electrical double layer at a semiconductor/electrolyte interface make the EGOFETs practical as biosensors for the quantification of C-reactive protein (CRP) and bisphenol A (BPA).^[264] Although FET-based biosensors offer impressive sensitivity for protein detection, the performance can be severely affected by the ion strength of the samples. Thorough deionization steps are essentially needed to enable this technology for single-cell protein analysis using real physiological conditions.

3.3.3. Impedance-Based Protein Detection

Electrochemical impedance spectroscopy (EIS) is a technique that measures the electrical impedance of an interface in the AC steady state with constant DC bias conditions.^[271] EIS-based

biosensors have been extensively exploited for label-free protein detection due to their low cost, simplicity, and rapid detection. They exert minimal damage to the biological samples by imposing a small sinusoidal voltage at a particular frequency as compared to other DC-based electrochemical methods. A representative EIS-based IFN- γ -sensor was illustrated by Min et al.^[272] The complex formation through aptamer-analyte interaction induced a change in charge-transfer resistance on the electrode surface. A detection limit of 100 fM was achieved in 10 mM sodium phosphate buffer with 5 mM [Fe(CN)₆]^{3-/4-}. Nevertheless, this aptasensor failed to detect IFN- γ in fetal bovine serum, suggesting the potential difficulty in translating this technology for practical biosensing applications. To this end, Kongsuphol et al. proposed an EIS-based TNF- α biosensor for direct detection in nondiluted human serum.^[273] With the aid of magnetic beads, the detection of TNF- α from nondiluted serum was realized in a three-step process: i) removal of abundant interfering proteins albumin and IgG antibodies by coupling of magnetic beads; ii) capture of magnetic beads functionalized with TNF- α by TNF- α -antibody; and iii) release and detection of TNF- α by the EIS technique. Although a relatively low detection limit of 1 pg mL⁻¹ was achieved, this technique lost the nature of EIS as a label-free biosensor with the need for tedious sample-preparation processes, thus not meeting the requirements for real-time single-cell protein analysis.

3.4. Optical Biosensors

Optical-biosensing techniques mainly operate with an optical transducer system by converting the receptor-analyte binding event into a light signal. These biosensors are performed by investigating the light interactions with a biorecognition element, allowing direct, real-time, and label-free detection of a variety of biological and chemical substances. They are less vulnerable to pH, ionic strength, or fluidic damping, which gives them a great advantage over electrochemical biosensors for single-cell protein analysis. In the following sections, we present the most commonly used configurations of optical biosensors.

3.4.1. Detection based on Photonic Crystals

Photonic crystals are dielectric-material-based periodic nanostructures that can trap light of a specific wavelength in a confined small volume by reflection.^[274] The deposition of target analytes on photonic crystals creates a local disruption of the periodicity and a symmetry of the crystal, inducing a variation in the reflection wavelength. Mandal et al. reported a one-dimensional photonic crystal array for a label-free and multiplexed biosensor (see Figure 6a).^[275] The photonic-crystal-resonator array was fabricated on a low-index SiO₂ substrate with 8 microcavities and a silicon waveguide. Multiplexed detection was enabled by engineering the photonic crystal arrays at different cavity distances, with each of them showing a characteristic resonant wavelength. Photonic-crystal fiber, which consists of periodically and axially aligned air channels along the entire fiber, has also been applied in protein biosensing.^[276,277] More

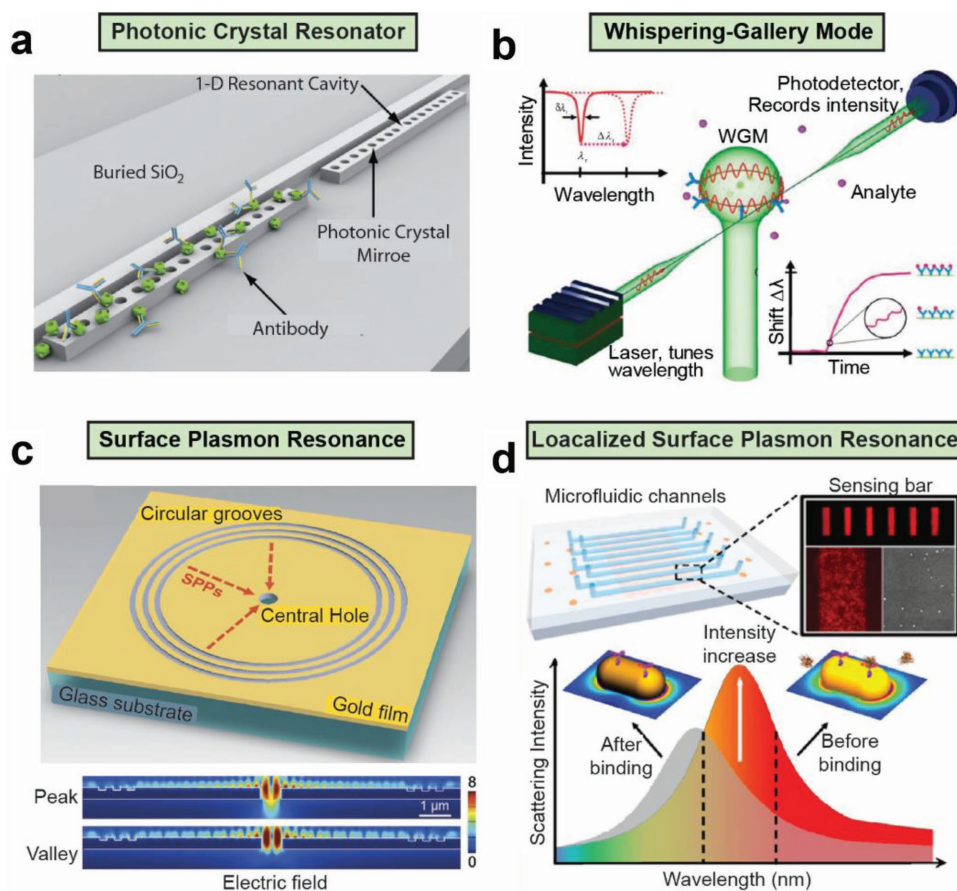


Figure 6. Optical technologies that enable quantification of cell secretomics at the single-cell level. a) Demonstration of one-dimensional photonic-crystal resonator arrays functionalized with antigens, and without antigens. Reproduced with permission.^[275] Copyright 2009, The Royal Society of Chemistry. b) Concept of whispering-gallery-mode-based biosensing. Analyte-binding-events-induced optical-path-length increase, changing the resonance wavelength. Reproduced with permission.^[279] Copyright 2008, Nature Publishing Group. c) Illustration of plasmonic interferometer. A gold array of a circular aperture–groove nanostructure was fabricated on a glass substrate to allow transmission detection of protein binding. Reproduced with permission.^[280] Copyright 2013, The Royal Society of Chemistry. d) The schematics of an LSPR nanoplasmonic microarray. Samples were loaded through the parallel microchannels to allow real-time, high-throughput, multiplex protein analysis by monitoring the scattering light intensity variation. Reproduced with permission.^[281] Copyright 2015, American Chemical Society.

recently, a handheld photonic-crystal imaging biosensor was developed that can provide a parallel, label-free, time-resolved detection of CD40 ligand antibody, EGF antibody, and streptavidin.^[278] Photonic-crystal biosensors typically exhibit superior sensitivity for protein detection empowered by the high quality factor of the perfectly arranged structure. The potential challenges that lie ahead for single-cell secretomics are the scalability of the sensor fabrication and the sophisticated optical-setup requirements.

3.4.2. Detection based on the Whispering-Gallery-Mode

Optical whispering-gallery-mode (WGM)-based biosensing relies on the light confinement within a glass sphere through continuous total internal reflection (Figure 6b).^[279] When the optical path length is an integer multiple of the wavelength, resonance occurs, to yield a dip in the light intensity transmitted. The binding of target molecules on the sphere increases this path length, which can be characterized by a redshift at a

given resonant frequency. A WGM-based biosensor was first proposed by Vollmer et al. for the detection of BSA.^[282] In their study, a biotin-functionalized silica glass microsphere was immobilized in the center of the sample room and connected with an optical fiber. The binding of streptavidin on the biotinylated microsphere increased the effective radius and the resulting resonance drift was monitored in real time by a photodetector. Single-molecule detection of interleukin-2 (IL-2) was achieved by improving the quality factor (Q) of the system to $\approx 10^8$.^[283] Multiplexed WGM-based detection was recently demonstrated by using barium titanate microspheres with different diameters.^[284] Simultaneous quantification of multiple oral-cancer biomarkers was achieved by exciting and imaging over 120 microsphere resonators with a relatively good limit of detection at $\approx 100 \text{ pg mL}^{-1}$. Further improvement in the sensitivity of this technology in a highly multiplex scheme will make it promising for real-time single-cell secretomics.

Optical ring resonators use the same concept as behind the WGM except by manipulating light following the principles of constructive interference and total internal reflection.

Luchansky and Bailey proposed a silicon micro-ring-resonator-array based immunosensor for the label-free detection of cell-secreted cytokines.^[285] Primary antibodies were first added into the cell culture media and then attached onto the micro-ring-resonator array. Corresponding analyte binding to a specific array of the antibody pre-immobilized sensor surface altered the resonance wavelength. Interestingly, the quantification of the analyte was based on the initial slope of the real-time binding curve during the first 5 min of the experiment. This method offers a remarkable sensor turn-around time, which can be broadly applied to other types of label-free, real-time biosensors for rapid quantification of protein secretion from individual cells.

3.4.3. Plasmonics-Based Detection

Surface plasmon resonance (SPR) is an optical phenomenon on a noble-metal surface that provides a label-free, non-invasive means for biomolecule detection. SPR generates a propagating evanescent wave on the metal surface, which is highly sensitive to the local change of refractive index.^[286] The penetration depth of the evanescent field decays exponentially with the distance away from the sensor surface. Thus, SPR techniques have been predominantly applied in studying biomolecule surface binding, analyte–antibody binding affinity, protein–protein interactions, and cell detection.^[287–295] SPR biosensors usually employ the conventional Kretschmann configuration that requires bulky optical equipment, posing a significant challenge for system miniaturization. Motivated by this concern, an integrated microfluidic SPR biosensor was demonstrated by Luo et al., which allowed high-throughput, real-time measurements of immunoreaction with drastically reduced assay time and sample volume.^[296] Ouellet et al. also demonstrated a parallel microfluidic SPR array with 264 incubation microchambers for rapid, high-throughput determination of antibody–analyte binding affinities.^[291] Recent development of the SPR platform consisting of an array of circular aperture–groove nanostructures further simplified the system (Figure 6c).^[280] Based on the well-known “bull’s eye” structure, the BSA–anti-BSA binding was characterized by the relative intensity change of the transmission light. SPR-based biosensors possess unique advantages for high-throughput, real-time, multiplexed protein-binding analysis.^[297] The new sensing structure design and surface function process with better sensitivity and reduced nonspecific binding will greatly facilitate the transformation of this technology for single-cell protein detection.

Localized surface plasmon resonance (LSPR) occurs at the interface between a noble nanoparticle and its surrounding medium upon light illumination at a certain wavelength. The resonant electron oscillation generates a dramatically enhanced local electromagnetic field on the nanoparticle surface, which is extremely sensitive to the environmental change in the surrounding medium (with 5–10 nm of the nanoparticle surface).^[298] LSPR-based biosensors have attracted enormous attention in the past few decades due to their exceptional sensing capability and compatibility for miniaturization and integration. Malinsky et al. proposed the first LSPR biosensor

utilizing silver nanoparticles as the sensing elements.^[299] Since then, this technique has been expanded and applied in the detection of a wide variety of biomolecules.^[300–305] A significant amount of effort has been devoted to improving the performance of LSPR biosensors. Early theoretical prediction by Chen et al. revealed the role of the nanoparticle geometry in affecting the sensor sensitivity.^[306] Various shapes of noble-metal nanoparticles have been investigated, such as gold nanospheres, gold nanorods, gold nanodiscs, gold nano-bipyramids, gold nanocrescents, silver nanoprisms, silver nanotriangles.^[281,304,307–313] The importance of nanoparticle orientation and the polarization of the incident light was further studied by Mayer et al.^[313] LSPR biosensors can be easily integrated with microfluidic devices to achieve efficient sample spraying and real-time measurements.^[308] Notably, the majority of the conventional LSPR biosensors adopt the spectrum-shift-based detection scheme, intrinsically limiting the accuracy and throughput of this technology.^[305,312] To overcome this limitation, Chen et al. reported an LSPR dark-field imaging technique that enabled a massive, parallel multiplexed serum immunoassay by measuring the scattering intensity change of patterned gold-nanorod microarrays (Figure 6d).^[281] This technique was implemented to quantitatively characterize the dynamic protein-secretion response of antigen-stimulated Jurkat cells exposed to an immunosuppressive agent tacrolimus.^[304] Very recently, Song et al. integrated an AC electro-osmosis flow with the LSPR imaging technique that further improved the sensitivity of IL-1 β in human serum down to 1 pg mL⁻¹ with a reduced assay time of 5 min.^[314] The demonstrated capabilities of this LSPR platform render it a promising candidate for rapid, high-throughput, multi-parametric protein analysis toward single-cell secretomics.

4. Integrated Microfluidic Biosensing Systems toward Real-Time Single-Cell Secretomics

Creation of an integrated microfluidic biosensing system incorporating both the aspects of single-cell isolation/manipulation and real-time single-cell protein sensing increases the level of complexity and poses significant technical challenges. However, so far, there have been limited numbers of such integrated systems reported, primarily using static measurements. Fan et al. demonstrated a DNA-encoded antibody library (DEAL) technique for single-cell multiplexed plasma-protein detection using valve-controlled microfluidic channels.^[315] By using this sensing technique, Ma et al. demonstrated a single-cell barcode chip (SCBC) for quantitative determination of cytokine secretion of lipopolysaccharide (LPS)-stimulated THP-1 human macrophage (see Figure 7a).^[22] Although the aforementioned studies offer on-chip protein analysis at single-cell resolution, temporal secretion information is unfortunately missing owing to the long assay time of the labeling sensing techniques. In order to obtain the temporal secretion information from single cells, Han et al. attempted a microengraving method coupling a dense array of microwells, and sandwich-based ELISA was used to measure the time-dependent (every 2 h) cytokine-secretion profile for understanding the polyfunctional response of T-cells (see Figure 7b).^[316] Other attempts have also been

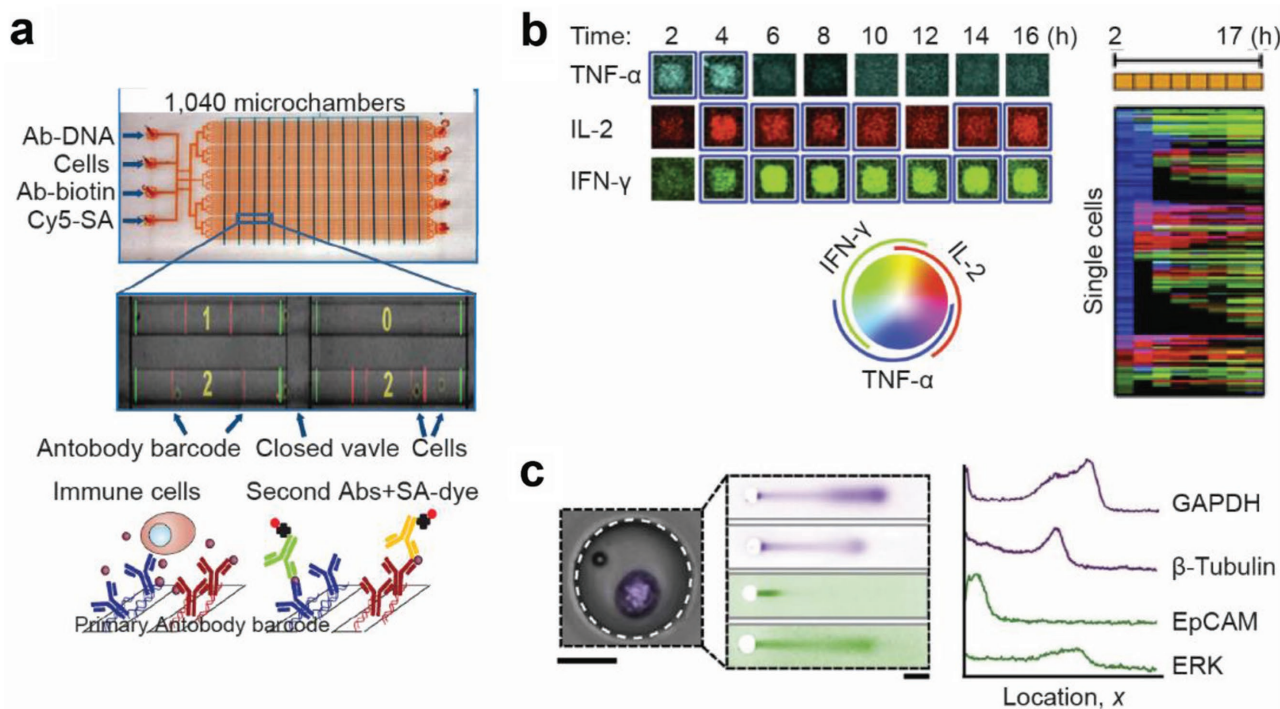


Figure 7. Integrated single-cell sensing platforms that combine both cell manipulation and biosensing. a) Design of multiplexed detection of plasma proteins from single cells in a microfluidics-based chip using DNA-encoded antibody barcode arrays. Reproduced with permission.^[22] Copyright 2011, Nature Publishing Group. b) Integrated microwell-based sensing system for polyfunctional analysis of T-cell cytokine secretion dynamics. The top-left image shows representative microscopy images of temporal cytokine measurement of TNF α (blue), IL-2 (red), and IFN- γ (green) secretion from single T cells. The top-right image shows the array of cytokine secretion kinetics of viable T cells. The bottom-left color-wheel image illustrates the type and relative magnitude of secreted cytokines. Reproduced with permission.^[316] Copyright 2012, National Academy of Sciences of the USA. c) Single CTCs isolated from whole blood sample were individually deposited in each microwells (left). Multiple proteins were separated by PAGE (middle), and analyzed by Western blotting (right). Reproduced with permission.^[318] Copyright 2017, Nature Publishing Group.

made to integrate label-free amperometric biosensors with a microfluidic cell capture system for accessing the dynamic information on cellular secretion.^[260,317] More recently, a new platform that integrated vortex technology for isolation of CTCs from whole blood with polyacrylamide gel electrophoresis (PAGE) for analysis of multiple proteins was proposed by Sinkala et al. (see Figure 7c)^[318] Another exciting study that has enabled label-free detection of single *E. coli* cell secreted proteins with a fine temporal and spatial resolution has also been demonstrated by Landry et al.^[319] All these studies exemplify the integrated systems for on-chip cellular analysis and provide great insights for a new generation of microfluidic biosensing systems toward real-time single-cell secretomics.

5. Conclusion

Microfluidic tools, such as droplet microfluidics, microwell arrays, and valve microfluidics, offer new opportunities for spatial confinement of discrete individual cells or co-cultures. The simplicity, ease of use, and flexibility for integration make these platforms propitious for integrated microfluidic single-cell biosensing. Similarly, label-free biosensors exhibiting excellent sensing performance, high degree of compatibility, and great capability for miniaturization would be poised for

complementing the microtools for single-cell biosensing. Synergistic combination of these two components into an integrated microfluidic biosensing system will make it feasible to access the dynamic functional response and intracellular signaling at single-cell resolution. We envision the use of such a platform for the analysis of single-cell secretomics will close the knowledge gap in understanding the cellular phenotype and functional heterogeneity and expand exponentially in fundamental research and clinical applications. Further development of such integrated systems would ultimately gear biologists and clinicians with new tools for rapid disease diagnosis and screening, identification of rare cell populations, novel drug discovery, and precise therapeutic treatment.

Acknowledgements

The authors acknowledge financial support from the New York University Department of Mechanical and Aerospace Engineering, the New York University Global Seed Grant, the Auburn University Department of Mechanical Engineering and Detection and Food Safety Center.

Conflict of Interest

The authors declare no conflict of interest.

Keywords

biosensing, cell secretomics, microfluidics, proteins, single-cell analysis

Received: May 17, 2017

Revised: June 15, 2017

Published online:

- [1] D. D. Carlo, L. P. Lee, *Anal. Chem.* **2006**, *78*, 7918.
- [2] B. S. Davis, G.-J. J. Chang, B. Cropp, J. T. Roehrig, D. A. Martin, C. J. Mitchell, R. Bowen, M. L. Bunning, *J. Virol.* **2001**, *75*, 4040.
- [3] E. Engvall, P. Perlmann, *J. Immunol.* **1972**, *109*, 129.
- [4] T. Lion, A. Gaiger, T. Henn, E. Hörth, O. Haas, K. Geissler, H. Gadner, *Leukemia* **1995**, *9*, 1353.
- [5] D. A. Martin, D. A. Muth, T. Brown, A. J. Johnson, N. Karabatsos, J. T. Roehrig, *J. Clin. Microbiol.* **2000**, *38*, 1823.
- [6] F. Delvigne, P. Goffin, *Biotechnol. J.* **2014**, *9*, 61.
- [7] A. Grünberger, W. Wiechert, D. Kohlheyer, *Curr. Opin. Biotechnol.* **2014**, *29*, 15.
- [8] H. Yin, D. Marshall, *Curr. Opin. Biotechnol.* **2012**, *23*, 110.
- [9] A. Amantonico, P. L. Urban, R. Zenobi, *Anal. Bioanal. Chem.* **2010**, *398*, 2493.
- [10] T. Kalisky, S. R. Quake, *Nat. Methods* **2011**, *8*, 311.
- [11] A. Salehi-Reyhani, J. Kaplinsky, E. Burgin, M. Novakova, R. H. Templer, P. Parker, M. A. Neil, O. Ces, P. French, K. R. Willison, *Lab Chip* **2011**, *11*, 1256.
- [12] A. K. Shalek, R. Satija, X. Adiconis, R. S. Gertner, J. T. Gaublonne, R. Raychowdhury, S. Schwartz, N. Yosef, C. Malboeuf, D. Lu, *Nature* **2013**, *498*, 236.
- [13] N. Navin, J. Hicks, *Genome Med.* **2011**, *3*, 31.
- [14] A. G. Brolo, *Nat. Photonics* **2012**, *6*, 709.
- [15] P. K. Chattopadhyay, T. M. Gierahn, M. Roederer, J. C. Love, *Nat. Immunol.* **2014**, *15*, 128.
- [16] W. Zhao, S. Schafer, J. Choi, Y. J. Yamanaka, M. L. Lombardi, S. Bose, A. L. Carlson, J. A. Phillips, W. Teo, I. A. Droujinine, *Nat. Nanotechnol.* **2011**, *6*, 524.
- [17] L. Cai, N. Friedman, X. S. Xie, *Nature* **2006**, *440*, 358.
- [18] K. Eyer, P. Kuhn, C. Hanke, P. S. Dittrich, *Lab Chip* **2012**, *12*, 765.
- [19] L. Novotny, R. X. Bian, X. S. Xie, *Phys. Rev. Lett.* **1997**, *79*, 645.
- [20] X. Wang, S. Chen, M. Kong, Z. Wang, K. D. Costa, R. A. Li, D. Sun, *Lab Chip* **2011**, *11*, 3656.
- [21] L. D. Giavedoni, *J. Immunol. Methods* **2005**, *301*, 89.
- [22] C. Ma, R. Fan, H. Ahmad, Q. Shi, B. Comin-Anduix, T. Chodon, R. C. Koya, C.-C. Liu, G. A. Kwong, C. G. Radu, *Nat. Med.* **2011**, *17*, 738.
- [23] L. Mendoza, R. McQuary, A. Mongan, R. Gangadharan, S. Brignac, M. Eggers, *BioTechniques* **1999**, *27*, 778.
- [24] S. M. Borisov, O. S. Wolfbeis, *Chem. Rev.* **2008**, *108*, 423.
- [25] E. Azuaje-Hualde, M. García-Hernando, J. Etxebarria-Elezgarai, M. M. D. Pancorbo, F. Benito-Lopez, L. Basabe-Desmonts, *Micromachines* **2017**, *8*, 166.
- [26] S. Ishii, K. Tago, K. Senoo, *Appl. Microbiol. Biotechnol.* **2010**, *86*, 1281.
- [27] J. Nilsson, M. Evander, B. Hammarström, T. Laurell, *Anal. Chim. Acta* **2009**, *649*, 141.
- [28] H. Zhang, K.-K. Liu, *J. R. Soc. Interface* **2008**, *5*, 671.
- [29] S. L. Anna, N. Bontoux, H. A. Stone, *Appl. Phys. Lett.* **2003**, *82*, 364.
- [30] E. Brouzes, M. Medkova, N. Savenelli, D. Marran, M. Twardowski, J. B. Hutchison, J. M. Rothberg, D. R. Link, N. Perrimon, M. L. Samuels, *Proc. Natl. Acad. Sci. USA* **2009**, *106*, 14195.
- [31] M. T. Guo, A. Rotem, J. A. Heyman, D. A. Weitz, *Lab Chip* **2012**, *12*, 2146.
- [32] A. Huebner, S. Sharma, M. Srisa-Art, F. Hollfelder, J. B. Edel, *Lab Chip* **2008**, *8*, 1244.
- [33] P. Kumaresan, C. J. Yang, S. A. Cronier, R. G. Blazej, R. A. Mathies, *Anal. Chem.* **2008**, *80*, 3522.
- [34] W. Liu, H. J. Kim, E. M. Lucchetta, W. Du, R. F. Ismagilov, *Lab Chip* **2009**, *9*, 2153.
- [35] V. Taly, B. T. Kelly, A. D. Griffiths, *ChemBioChem* **2007**, *8*, 263.
- [36] D. S. Tawfik, A. D. Griffiths, *Nat. Biotechnol.* **1998**, *16*, 652.
- [37] T. Thorsen, R. W. Roberts, F. H. Arnold, S. R. Quake, *Phys. Rev. Lett.* **2001**, *86*, 4163.
- [38] A. M. Klein, L. Mazutis, I. Akartuna, N. Tallapragada, A. Veres, V. Li, L. Peshkin, D. A. Weitz, M. W. Kirschner, *Cell* **2015**, *161*, 1187.
- [39] P. Garstecki, M. J. Fuerstman, H. A. Stone, G. M. Whitesides, *Lab Chip* **2006**, *6*, 437.
- [40] D. Link, S. L. Anna, D. Weitz, H. Stone, *Phys. Rev. Lett.* **2004**, *92*, 054503.
- [41] G. F. Christopher, S. L. Anna, *J. Phys. D: Appl. Phys.* **2007**, *40*, R319.
- [42] R. Zilionis, J. Nainys, A. Veres, V. Savova, D. Zemmour, A. M. Klein, L. Mazutis, *Nat. Protoc.* **2017**, *12*, 44.
- [43] M. Chabert, J.-L. Viovy, *Proc. Natl. Acad. Sci. USA* **2008**, *105*, 3191.
- [44] T. P. Lagus, J. F. Edd, *J. Phys. D: Appl. Phys.* **2013**, *46*, 114005.
- [45] J. Clausell-Tormos, D. Lieber, J.-C. Baret, A. El-Harrak, O. J. Miller, L. Frenz, J. Blouwolfk, K. J. Humphry, S. Köster, H. Duan, *Chem. Biol.* **2008**, *15*, 427.
- [46] A. Huebner, M. Srisa-Art, D. Holt, C. Abell, F. Hollfelder, J. Edel, *Chem. Commun.* **2007**, 1218.
- [47] M. He, J. S. Edgar, G. D. Jeffries, R. M. Lorenz, J. P. Shelby, D. T. Chiu, *Anal. Chem.* **2005**, *77*, 1539.
- [48] J.-C. Baret, O. J. Miller, V. Taly, M. Ryckelynck, A. El-Harrak, L. Frenz, C. Rick, M. L. Samuels, J. B. Hutchison, J. J. Agresti, *Lab Chip* **2009**, *9*, 1850.
- [49] A. Fallah-Araghi, J.-C. Baret, M. Ryckelynck, A. D. Griffiths, *Lab Chip* **2012**, *12*, 882.
- [50] L. Mazutis, J. Gilbert, W. L. Ung, D. A. Weitz, A. D. Griffiths, J. A. Heyman, *Nat. Protoc.* **2013**, *8*, 870.
- [51] H. Hufnagel, A. Huebner, C. Gülch, K. Güse, C. Abell, F. Hollfelder, *Lab Chip* **2009**, *9*, 1576.
- [52] Y.-C. Tan, J. S. Fisher, A. I. Lee, V. Cristini, A. P. Lee, *Lab Chip* **2004**, *4*, 292.
- [53] W. Bonner, H. Hulett, R. Sweet, L. Herzenberg, *Rev. Sci. Instrum.* **1972**, *43*, 404.
- [54] A. Wolff, I. R. Perch-Nielsen, U. D. Larsen, P. Friis, G. Goranovic, C. R. Poulsen, J. R. P. Kutter, P. Telleman, *Lab Chip* **2003**, *3*, 22.
- [55] S. Köster, F. E. Angile, H. Duan, J. J. Agresti, A. Wintner, C. Schmitz, A. C. Rowat, C. A. Merten, D. Pisignano, A. D. Griffiths, *Lab Chip* **2008**, *8*, 1110.
- [56] M. J. Fulwyler, R. B. Glascock, R. D. Hiebert, N. M. Johnson, *Rev. Sci. Instrum.* **1969**, *40*, 42.
- [57] R. G. Sweet, *Rev. Sci. Instrum.* **1965**, *36*, 131.
- [58] B. Liesegang, A. Radbruch, K. Rajewsky, *Proc. Natl. Acad. Sci. USA* **1978**, *75*, 3901.
- [59] G. P. Nolan, S. Fiering, J.-F. Nicolas, L. A. Herzenberg, *Proc. Natl. Acad. Sci. USA* **1988**, *85*, 2603.
- [60] R. H. Cole, N. de Lange, Z. J. Gartner, A. R. Abate, *Lab Chip* **2015**, *15*, 2754.
- [61] J. Martini, M. I. Recht, M. Huck, M. W. Bern, N. M. Johnson, P. Kiesel, *Lab Chip* **2012**, *12*, 5057.
- [62] B. L. Brizzard, R. Chubet, D. Vizard, *BioTechniques* **1994**, *16*, 730.
- [63] Y. Nakatani, V. Ogryzko, *Methods Enzymol.* **2003**, *370*, 430.
- [64] C. A. Bichsel, S. Gobaa, S. Kobel, C. Secondini, G. N. Thalmann, M. G. Cecchini, M. P. Lutolf, *Lab Chip* **2012**, *12*, 2313.
- [65] S. Wang, K. Liu, J. Liu, Z. T. F. Yu, X. Xu, L. Zhao, T. Lee, E. K. Lee, J. Reiss, Y. K. Lee, *Angew. Chem., Int. Ed.* **2011**, *50*, 3084.
- [66] S.-K. Lee, G.-S. Kim, Y. Wu, D.-J. Kim, Y. Lu, M. Kwak, L. Han, J.-H. Hyung, J.-K. Seol, C. Sander, *Nano Lett.* **2012**, *12*, 2697.

- [67] S. B. Carter, *Exp. Cell Res.* **1967**, *48*, 189.
- [68] A. Folch, M. Toner, *Annu. Rev. Biomed. Eng.* **2000**, *2*, 227.
- [69] J. Shay, K. Porter, T. Krueger, *Exp. Cell Res.* **1977**, *105*, 1.
- [70] K. Torimitsu, A. Kawana, *Dev. Brain Res.* **1990**, *51*, 128.
- [71] V. Plaks, C. D. Koopman, Z. Werb, *Science* **2013**, *341*, 1186.
- [72] F. A. Coumans, S. T. Ligthart, J. W. Uhr, L. W. Terstappen, *Clin. Cancer Res.* **2012**, *18*, 5711.
- [73] A. Barradas, L. W. Terstappen, *Cancers (Basel)* **2013**, *5*, 1619.
- [74] Y. Dong, A. M. Skelley, K. D. Merdek, K. M. Sprott, C. Jiang, W. E. Pierceall, J. Lin, M. Stocum, W. P. Carney, D. A. Smirnov, *J. Mol. Diagn.* **2013**, *15*, 149.
- [75] P. Li, Z. S. Stratton, M. Dao, J. Ritz, T. J. Huang, *Lab Chip* **2013**, *13*, 602.
- [76] S. Nagrath, L. V. Sequist, S. Maheswaran, D. W. Bell, D. Irimia, L. Ulkus, M. R. Smith, E. L. Kwak, S. Digumarthy, A. Muzikansky, *Nature* **2007**, *450*, 1235.
- [77] H. J. Yoon, T. H. Kim, Z. Zhang, E. Azizi, T. M. Pham, C. Paoletti, J. Lin, N. Ramnath, M. S. Wicha, D. F. Hayes, D. M. Simeone, S. Nagrath, *Nat. Nanotechnol.* **2013**, *8*, 735.
- [78] K. E. Schwab, P. Hutchinson, C. E. Gargett, *Hum. Reprod.* **2008**, *23*, 934.
- [79] Q. Zhou, K. Son, Y. Liu, A. Revzin, *Annu. Rev. Biomed. Eng.* **2015**, *17*, 170.
- [80] Q. Shen, L. Xu, L. Zhao, D. Wu, Y. Fan, Y. Zhou, W. O. Yang, X. Xu, Z. Zhang, M. Song, T. Lee, M. A. Garcia, B. Xiong, S. Hou, H. Tseng, X. Fang, *Adv. Mater.* **2013**, *25*, 2368.
- [81] F. Zheng, Y. Cheng, J. Wang, J. Lu, B. Zhang, Y. Zhao, Z. Gu, *Adv. Mater.* **2014**, *26*, 7333.
- [82] J. Kling, *Nat. Biotechnol.* **2012**, *30*, 578.
- [83] E. Sollier, D. E. Go, J. Che, D. R. Gossett, S. O'Byrne, W. M. Weaver, N. Kummer, M. Rettig, J. Goldman, N. Nickols, S. McCloskey, R. P. Kulkarni, D. D. Carlo, *Lab Chip* **2014**, *14*, 63.
- [84] A. M. Shah, M. Yu, Z. Nakamura, J. Ciciliano, M. Ulman, K. Kotz, S. L. Stott, S. Maheswaran, D. A. Haber, M. Toner, *Anal. Chem.* **2012**, *84*, 3682.
- [85] K. J. Son, A. Rahimian, D.-S. Shin, C. Siltanen, T. Patel, A. Revzin, *Analyst* **2016**, *141*, 679.
- [86] M. Charnley, M. Textor, A. Khademhosseini, M. P. Lutolf, *Integr. Biol.* **2009**, *1*, 625.
- [87] H. Kim, J. Doh, D. J. Irvine, R. E. Cohen, P. T. Hammond, *Biomacromolecules* **2004**, *5*, 822.
- [88] S. Lindström, H. Andersson-Svahn, *Lab Chip* **2010**, *10*, 3363.
- [89] E. Ostuni, C. S. Chen, D. E. Ingber, G. M. Whitesides, *Langmuir* **2001**, *17*, 2828.
- [90] D. K. Wood, D. M. Weingeist, S. N. Bhatia, B. P. Engelward, *Proc. Natl. Acad. Sci. USA* **2010**, *107*, 10008.
- [91] A. Revzin, R. G. Tompkins, M. Toner, *Langmuir* **2003**, *19*, 9855.
- [92] J. R. Rettig, A. Folch, *Anal. Chem.* **2005**, *77*, 5628.
- [93] J. J. Kim, K. W. Bong, E. Reátegui, D. Irimia, P. S. Doyle, *Nat. Mater.* **2017**, *16*, 139.
- [94] K. J. Son, D.-S. Shin, T. Kwa, J. You, Y. Gao, A. Revzin, *Lab Chip* **2015**, *15*, 637.
- [95] B. Dykstra, J. Ramunas, D. Kent, L. McCaffrey, E. Szumsky, L. Kelly, K. Farn, A. Blaylock, C. Eaves, E. Jervis, *Proc. Natl. Acad. Sci. USA* **2006**, *103*, 8185.
- [96] V. r. Lecault, M. VanInsberghe, S. Sekulovic, D. J. H. F. Knapp, S. Wohrer, W. Bowden, F. Viel, T. McLaughlin, A. Jarandehi, M. Miller, *Nat. Methods* **2011**, *8*, 581.
- [97] A. Khademhosseini, R. Langer, J. Borenstein, J. P. Vacanti, *Proc. Natl. Acad. Sci. USA* **2006**, *103*, 2480.
- [98] A. Ashkin, *Science* **1980**, *210*, 1081.
- [99] S. Chu, J. E. Bjorkholm, A. Ashkin, A. Cable, *Phys. Rev. Lett.* **1986**, *57*, 314.
- [100] A. Ashkin, *IEEE J. Sel. Top. Quantum Electron.* **2000**, *6*, 841.
- [101] A. Ashkin, *Phys. Rev. Lett.* **1978**, *40*, 729.
- [102] D. G. Grier, *Nature* **2003**, *424*, 810.
- [103] K. C. Neuman, A. Nagy, *Nat. Methods* **2008**, *5*, 491.
- [104] A. Ashkin, J. M. Dziedzic, J. E. Bjorkholm, S. Chu, *Opt. Lett.* **1986**, *11*, 288.
- [105] A. Ashkin, J. M. Dziedzic, *Science* **1987**, *235*, 1517.
- [106] A. Ashkin, J. M. Dziedzic, *Proc. Natl. Acad. Sci. USA* **1989**, *86*, 7914.
- [107] A. Ashkin, J. M. Dziedzic, T. Yamane, *Nature* **1987**, *330*, 769.
- [108] S. M. Block, D. F. Blair, H. C. Berg, *Cytometry* **1991**, *12*, 492.
- [109] H. Liang, W. H. Wright, S. Cheng, W. He, M. W. Berns, *Exp. Cell Res.* **1993**, *204*, 110.
- [110] Y. Tadir, W. H. Wright, O. Vafa, T. Ord, R. H. Asch, M. W. Berns, *Fertil. Steril.* **1989**, *52*, 870.
- [111] H. Yin, M. D. Wang, K. Svoboda, R. Landick, *Science* **1995**, *270*, 1653.
- [112] W. Wang, Y. Liu, G. J. Sonek, M. W. Berns, R. A. Keller, *Appl. Phys. Lett.* **1995**, *67*, 1057.
- [113] C.-C. Lin, A. Chen, C.-H. Lin, *Biomed. Microdevices* **2008**, *10*, 55.
- [114] M. P. MacDonald, G. C. Spalding, K. Dholakia, *Nature* **2003**, *426*, 421.
- [115] M. M. Wang, E. Tu, D. E. Raymond, J. M. Yang, H. Zhang, N. Hagen, B. Dees, E. M. Mercer, A. H. Forster, I. Kariv, *Nat. Biotechnol.* **2005**, *23*, 83.
- [116] R. W. Applegate Jr, J. Squier, T. Vestad, J. Oakey, D. W. M. Marr, P. Bado, M. A. Dugan, A. A. Said, *Lab Chip* **2006**, *6*, 422.
- [117] T. D. Perroud, J. N. Kaiser, J. C. Sy, T. W. Lane, C. S. Branda, A. K. Singh, K. D. Patel, *Anal. Chem.* **2008**, *80*, 6365.
- [118] F. Arai, C. Ng, H. Maruyama, A. Ichikawa, H. El-Shimy, T. Fukuda, *Lab Chip* **2005**, *5*, 1399.
- [119] C. T. Lim, M. Dao, S. Suresh, C. H. Sow, K. T. Chew, *Acta Mater.* **2004**, *52*, 1837.
- [120] M. D. Wang, H. Yin, R. Landick, J. Gelles, S. M. Block, *Biophys. J.* **1997**, *72*, 1335.
- [121] E. Eriksson, K. Sott, F. Lundqvist, M. Sveningsson, J. Scrimgeour, D. Hanstorp, M. Goksör, A. Graneli, *Lab Chip* **2010**, *10*, 617.
- [122] E. Eriksson, J. Enger, B. Nordlander, N. Erjavec, K. Ramser, M. Goksör, S. Hohmann, T. Nyström, D. Hanstorp, *Lab Chip* **2007**, *7*, 71.
- [123] M. L. Juan, M. Righini, R. Quidant, *Nat. Photonics* **2011**, *5*, 349.
- [124] M. Tanase, N. Biais, M. Sheetz, *Methods Cell Biol.* **2007**, *83*, 473.
- [125] N. Pamme, *Lab Chip* **2006**, *6*, 24.
- [126] I. Šafařík, M. Šafaříková, *J. Chromatogr., B: Biomed. Sci. Appl.* **1999**, *722*, 33.
- [127] C. Wilhelm, F. Gazeau, J. Roger, J. N. Pons, J. C. Bacri, *Langmuir* **2002**, *18*, 8148.
- [128] V. r. M. Laurent, S. Hénon, E. Planus, R. Fodil, M. Bolland, D. Isabey, F. O. Gallet, *J. Biomech. Eng.* **2002**, *124*, 408.
- [129] T. R. Strick, J. F. Allemand, D. Bensimon, V. Croquette, *Biophys. J.* **1998**, *74*, 2016.
- [130] S. B. Smith, L. Finzi, C. Bustamante, *Science* **1992**, *258*, 1122.
- [131] F. Ziemann, J. Rädler, E. Sackmann, *Biophys. J.* **1994**, *66*, 2210.
- [132] W. Möller, I. Nemoto, T. Matsuzaki, T. Hofer, J. Heyder, *Biophys. J.* **2000**, *79*, 720.
- [133] B. G. Hosu, K. Jakob, P. Bánki, F. I. Tóth, G. Forgacs, *Rev. Sci. Instrum.* **2003**, *74*, 4158.
- [134] A. R. Bausch, W. Möller, E. Sackmann, *Biophys. J.* **1999**, *76*, 573.
- [135] N. Wang, J. P. Butler, D. E. Ingber, *Science* **1993**, *260*, 1124.
- [136] A. H. B. de Vries, B. E. Krenn, R. van Driel, J. S. Kanger, *Biophys. J.* **2005**, *88*, 2137.
- [137] F. G. Schmidt, B. Hinner, E. Sackmann, *Phys. Rev. E* **2000**, *61*, 5646.
- [138] C.-H. Wu, Y.-Y. Huang, P. Chen, K. Hoshino, H. Liu, E. P. Frenkel, J. X. J. Zhang, K. V. Sokolov, *ACS Nano* **2013**, *7*, 8816.
- [139] J. C. Rife, M. M. Miller, P. E. Sheehan, C. R. Tamanaha, M. Tondra, L. J. Whitman, *Sens. Actuators, A* **2003**, *107*, 209.

- [140] S. Katsura, T. Yasuda, K. Hirano, A. Mizuno, S. Tanaka, *Supercond. Sci. Technol.* **2001**, *14*, 1131.
- [141] M. M. Miller, P. E. Sheehan, R. L. Edelstein, C. R. Tamanaha, L. Zhong, S. Bounnak, L. J. Whitman, R. J. Colton, *J. Magn. Magn. Mater.* **2001**, *225*, 138.
- [142] H. A. Ferreira, D. L. Graham, P. Parracho, V. n. Soares, P. P. Freitas, *IEEE Trans. Magn.* **2004**, *40*, 2652.
- [143] D. L. Graham, H. A. Ferreira, N. Feliciano, P. P. Freitas, L. A. Clarke, M. D. Amaral, *Sens. Actuators, B* **2005**, *107*, 936.
- [144] L. Ejsing, M. F. Hansen, A. K. Menon, H. A. Ferreira, D. L. Graham, P. P. Freitas, *J. Magn. Magn. Mater.* **2005**, *293*, 677.
- [145] L. Ejsing, M. F. Hansen, A. K. Menon, H. A. Ferreira, D. L. Graham, P. P. Freitas, *Appl. Phys. Lett.* **2004**, *84*, 4729.
- [146] L. Chang, M. Howdysheal, W.-C. Liao, C.-L. Chiang, D. Gallego-Perez, Z. Yang, W. Lu, J. C. Byrd, N. Muthusamy, L. J. Lee, *Small* **2015**, *11*, 1818.
- [147] R. Pethig, *Biomicrofluidics* **2010**, *4*, 022811.
- [148] J. Voldman, M. Toner, M. L. Gray, M. A. Schmidt, *J. Electrostatics* **2003**, *57*, 69.
- [149] M. P. Hughes, H. Morgan, *J. Phys. D: Appl. Phys.* **1998**, *31*, 2205.
- [150] B. M. Taff, J. Voldman, *Anal. Chem.* **2005**, *77*, 7976.
- [151] X. B. Wang, Y. Huang, J. P. H. Burt, G. H. Markx, R. Pethig, *J. Phys. D: Appl. Phys.* **1993**, *26*, 1278.
- [152] T. Schnelle, R. Hagedorn, G. Fuhr, S. Fiedler, T. Müller, *Biochim. Biophys. Acta, Gen. Subj.* **1993**, *1157*, 127.
- [153] F. Grom, J. R. Kentsch, T. Müller, T. Schnelle, M. Stelzle, *Electrophoresis* **2006**, *27*, 1386.
- [154] J. Yang, Y. Huang, X.-B. Wang, F. F. Becker, P. R. C. Gascoyne, *Anal. Chem.* **1999**, *71*, 911.
- [155] I. F. Cheng, V. E. Froude, Y. Zhu, H.-C. Chang, H.-C. Chang, *Lab Chip* **2009**, *9*, 3193.
- [156] A. Menachery, R. Pethig, *IEE Proc.: Nanobiotechnol.* **2005**, *152*, 145.
- [157] M. Elitas, N. Dhar, K. Schneider, A. Valero, T. Braschler, J. D. McKinney, P. Renaud, *Biomed. Phys. Eng. Express* **2017**, *3*, 2057.
- [158] H. Morgan, N. G. Green, *J. Electrostatics* **1997**, *42*, 279.
- [159] H. Li, R. Bashir, *Sens. Actuators, B* **2002**, *86*, 215.
- [160] A. Menachery, D. Graham, S. M. Messerli, R. Pethig, P. J. S. Smith, *IET Nanobiotechnol.* **2011**, *5*, 1.
- [161] M. Washizu, O. Kurosawa, *IEEE Trans. Ind. Appl.* **1990**, *26*, 1165.
- [162] B. H. Lapizco-Encinas, R. V. Davalos, B. A. Simmons, E. B. Cummings, Y. Fintschenko, *J. Microbiol. Methods* **2005**, *62*, 317.
- [163] H. Morgan, M. P. Hughes, N. G. Green, *Biophys. J.* **1999**, *77*, 516.
- [164] C. L. Asbury, A. H. Diercks, G. Van Den Engh, *Electrophoresis* **2002**, *23*, 2658.
- [165] C. L. Asbury, G. Van Den Engh, *Biophys. J.* **1998**, *74*, 1024.
- [166] C. Prinz, J. O. Tegenfeldt, R. H. Austin, E. C. Cox, J. C. Sturm, *Lab Chip* **2002**, *2*, 207.
- [167] R. Pethig, M. S. Talary, *IET Nanobiotechnol.* **2007**, *1*, 2.
- [168] T. Heida, W. L. C. Rutten, E. Marani, *IEEE Trans. Biomed. Eng.* **2001**, *48*, 921.
- [169] A. Menachery, N. Kumawat, M. Qasaimeh, *TrAC, Trends Anal. Chem.* **2017**, *89*, 1.
- [170] B. H. Lapizco-Encinas, S. Ozuna-Chacón, M. Rito-Palomares, *J. Chromatogr., A* **2008**, *1206*, 45.
- [171] T. P. Hunt, R. M. Westervelt, *Biomed. Microdevices* **2006**, *8*, 227.
- [172] H. Park, D. Kim, K.-S. Yun, *Sens. Actuators, B* **2010**, *150*, 167.
- [173] J. Shi, X. Mao, D. Ahmed, A. Colletti, T. J. Huang, *Lab Chip* **2008**, *8*, 221.
- [174] M. Tanyeri, E. M. Johnson-Chavarria, C. M. Schroeder, *Appl. Phys. Lett.* **2010**, *96*, 224101.
- [175] K. Yosioka, Y. Kawasima, *Acta Acust. Acust.* **1955**, *5*, 167.
- [176] M. Dyson, B. Woodward, J. B. Pond, *Nature* **1971**, *232*, 572.
- [177] N. V. Baker, *Nature* **1972**, *239*, 398.
- [178] W. T. Coakley, D. W. Bardsley, M. A. Grundy, F. Zamani, D. J. Clarke, *J. Chem. Technol. Biotechnol.* **1989**, *44*, 43.
- [179] H. M. Hertz, *J. Appl. Phys.* **1995**, *78*, 4845.
- [180] M. Evander, L. Johansson, T. Lilliehorn, J. Piskur, M. Lindvall, S. Johansson, M. Almqvist, T. Laurell, J. Nilsson, *Anal. Chem.* **2007**, *79*, 2984.
- [181] D. Bazou, L. A. Kuznetsova, W. T. Coakley, *Ultrasound Med. Biol.* **2005**, *31*, 423.
- [182] A. Neild, S. Oberti, G. Radziwill, J. r. Dual, *Biotechnol. Bioeng.* **2007**, *97*, 1335.
- [183] J. V. Norris, M. Evander, K. M. Horsman-Hall, J. Nilsson, T. Laurell, J. P. Landers, *Anal. Chem.* **2009**, *81*, 6089.
- [184] J. Shi, D. Ahmed, X. Mao, S.-C. S. Lin, A. Lawit, T. J. Huang, *Lab Chip* **2009**, *9*, 2890.
- [185] X. Ding, S.-C. S. Lin, B. Kiraly, H. Yue, S. Li, I. K. Chiang, J. Shi, S. J. Benkovic, T. J. Huang, *Proc. Natl. Acad. Sci. USA* **2012**, *109*, 11105.
- [186] T. Franke, S. Braunnüller, L. Schmid, A. Wixforth, D. A. Weitz, *Lab Chip* **2010**, *10*, 789.
- [187] M. Wiklund, S. Nilsson, H. M. Hertz, *J. Appl. Phys.* **2001**, *90*, 421.
- [188] M. Wiklund, P. Spégel, S. Nilsson, H. M. Hertz, *Ultrasonics* **2003**, *41*, 329.
- [189] G. I. Taylor, *Proc. R. Soc. Lond., Ser. A: Math., Phys. Charact.* **1934**, *146*, 501.
- [190] B. J. Bentley, L. G. Leal, *J. Fluid Mech.* **1986**, *167*, 219.
- [191] B. J. Bentley, L. G. Leal, *J. Fluid Mech.* **1986**, *167*, 241.
- [192] R. R. Lagnado, N. Phan-Thien, L. G. Leal, *Phys. Fluids* **1984**, *27*, 1094.
- [193] O. Scrivener, C. Berner, R. Cressely, R. Hocquart, R. Sellin, N. S. Vlachos, *J. Non-Newtonian Fluid Mech.* **1979**, *5*, 475.
- [194] J. A. Odell, A. Keller, Y. Rabin, *J. Chem. Phys.* **1988**, *88*, 4022.
- [195] Y. B. Bae, H. K. Jang, T. H. Shin, G. Phukan, T. T. Tran, G. Lee, W. R. Hwang, J. M. Kim, *Lab Chip* **2016**, *16*, 96.
- [196] W. Xu, S. J. Muller, *Lab Chip* **2012**, *12*, 647.
- [197] T. T. Perkins, D. E. Smith, S. Chu, *Science* **1997**, *276*, 2016.
- [198] R. Dylla-Spears, J. E. Townsend, L. Jen-Jacobson, L. L. Sohn, S. J. Muller, *Lab Chip* **2010**, *10*, 1543.
- [199] A. Ainla, I. Gözen, B. Hakonen, A. Jesorka, *Sci. Rep.* **2013**, *3*, 2743.
- [200] A. Sarkar, S. Koltitz, D. A. Lauffenburger, J. Han, *Nat. Commun.* **2014**, *5*,
- [201] G. V. Kaigala, R. D. Lovchik, E. Delamarche, *Angew. Chem., Int. Ed.* **2012**, *51*, 11224.
- [202] A. Ainla, G. D. M. Jeffries, R. Brune, O. Orwar, A. Jesorka, *Lab Chip* **2012**, *12*, 1255.
- [203] D. Juncker, H. Schmid, E. Delamarche, *Nat. Mater* **2005**, *4*, 622.
- [204] A. Kashyap, J. Autebert, E. Delamarche, G. V. Kaigala, *Sci. Rep.* **2016**, *6*,
- [205] M. Safavieh, M. A. Qasaimeh, A. Vakil, D. Juncker, T. Gervais, *Sci. Rep.* **2015**, *5*, 11943.
- [206] M. A. Qasaimeh, S. B. G. Ricoult, D. Juncker, *Lab Chip* **2013**, *13*, 40.
- [207] M. A. Qasaimeh, T. Gervais, D. Juncker, *Nat. Commun.* **2011**, *2*, 464.
- [208] A. T. Brimmo, M. A. Qasaimeh, *IEEE Nanotechnol. Mag.* **2017**, *11*, 20.
- [209] D. Di Carlo, D. Irimia, R. G. Tompkins, M. Toner, *Proc. Natl. Acad. Sci. USA* **2007**, *104*, 18892.
- [210] E. Ozkumur, A. M. Shah, J. C. Ciciliano, B. L. Emmink, D. T. Miyamoto, E. Brachtel, M. Yu, P.-i. Chen, B. Morgan, J. Trautwein, *Sci. Transl. Med.* **2013**, *5*, 179ra47.
- [211] H. W. Hou, M. E. Warkiani, B. L. Khoo, Z. R. Li, R. A. Soo, D. S.-W. Tan, W.-T. Lim, J. Han, A. A. S. Bhagat, C. T. Lim, *Sci. Rep.* **2013**, *3*, 1259.
- [212] W. R. Dean, *Philos. Mag.* **1928**, *5*, 673.

- [213] W. Al-Faqheri, T. H. G. Thio, M. A. Qasaimeh, A. Dietzel, M. Madou, A. Al-Halhouli, *Microfluid. Nanofluid.* **2017**, *21*, 102.
- [214] M. Yamada, M. Seki, *Lab Chip* **2005**, *5*, 1233.
- [215] X. Li, W. Chen, G. Liu, W. Lu, J. Fu, *Lab Chip* **2014**, *14*, 2565.
- [216] Q. D. Tran, T. F. Kong, D. Hu, R. H. W. Lam, *Lab Chip* **2016**, *16*, 2813.
- [217] B. Cetin, M. B. Özer, M. E. Solmaz, *Biochem. Eng. J.* **2014**, *92*, 63.
- [218] T. Thorsen, S. J. Maerkl, S. R. Quake, *Science* **2002**, *298*, 580.
- [219] I. E. Araci, P. Brisk, *Curr Opin Biotechnol* **2014**, *25*, 60.
- [220] H. C. Fan, J. Wang, A. Potanina, S. R. Quake, *Nat. Biotechnol* **2011**, *29*, 51.
- [221] J. M. T. Versteegen, T. Logtenberg, R. E. Ballieux, *J. Immunol. Methods* **1988**, *111*, 25.
- [222] T. T. MacDonald, P. Hutchings, M. Y. Choy, S. Murch, A. Cooke, *Clin. Exp. Immunol.* **1990**, *81*, 301.
- [223] J. C. Love, J. L. Ronan, G. M. Grotenbreg, A. G. van der Veen, H. L. Ploegh, *Nat. Biotechnol.* **2006**, *24*, 703.
- [224] A. Amantonico, P. L. Urban, S. R. Fagerer, R. M. Balabin, R. Zenobi, *Anal. Chem.* **2010**, *82*, 7394.
- [225] H. Li, X. Bai, N. Wang, X. Chen, J. Li, Z. Zhang, J. Tang, *Talanta* **2016**, *146*, 727.
- [226] M. Chen, H. Nam, H. Rokni, S. Wi, J. S. Yoon, P. Chen, K. Kurabayashi, W. Lu, X. Liang, *ACS Nano* **2015**, *9*, 8773.
- [227] B. Domon, R. Aebersold, *Science* **2006**, *312*, 212.
- [228] K. A. Tubbs, D. Nedelkov, R. W. Nelson, *Anal. Biochem.* **2001**, *289*, 26.
- [229] E. E. Niederkofler, K. A. Tubbs, K. Gruber, D. Nedelkov, U. A. Kiernan, P. Williams, R. W. Nelson, *Anal. Chem.* **2001**, *73*, 3294.
- [230] D. Yukihira, D. Miura, K. Saito, K. Takahashi, H. Wariishi, *Anal. Chem.* **2010**, *82*, 4278.
- [231] P. L. Urban, A. Amantonico, S. R. Fagerer, P. Gehrig, R. Zenobi, *Chem. Commun.* **2010**, *46*, 2212.
- [232] J. L. Edwards, R. T. Kennedy, *Anal. Chem.* **2005**, *77*, 2201.
- [233] M. Yang, T.-C. Chao, R. Nelson, A. Ros, *Anal. Bioanal. Chem.* **2012**, *404*, 1681.
- [234] K. Sugiyama, H. Harako, Y. Ukita, T. Shimoda, Y. Takamura, *Anal. Chem.* **2014**, *86*, 7593.
- [235] J. Han, J. Zhang, Y. Xia, S. Li, L. Jiang, *Colloids Surf., A* **2011**, *379*, 2.
- [236] F. Salam, Y. Uludag, I. E. Tothill, *Talanta* **2013**, *115*, 761.
- [237] H. J. Lee, K. Namkoong, E. C. Cho, C. Ko, J. C. Park, S. S. Lee, *Biosens. Bioelectron.* **2009**, *24*, 3120.
- [238] D. Lee, D. Kwon, W. Ko, J. Joo, H. Seo, S. S. Lee, S. Jeon, *Chem. Commun.* **2012**, *48*, 7182.
- [239] J. H. Lee, K. S. Hwang, J. Park, K. H. Yoon, D. S. Yoon, T. S. Kim, *Biosens. Bioelectron.* **2005**, *20*, 2157.
- [240] G. n. Sauerbrey, *Z. Phys.* **1959**, *155*, 206.
- [241] H. Sota, H. Yoshimine, R. F. Whittier, M. Gotoh, Y. Shinohara, Y. Hasegawa, Y. Okahata, *Anal. Chem.* **2002**, *74*, 3592.
- [242] R. Akter, C. K. Rhee, M. A. Rahman, *Biosens. Bioelectron.* **2015**, *66*, 539.
- [243] J. Lee, Y.-S. Choi, Y. Lee, H. J. Lee, J. N. Lee, S. K. Kim, K. Y. Han, E. C. Cho, J. C. Park, S. S. Lee, *Anal. Chem.* **2011**, *83*, 8629.
- [244] A. Numnuam, K. Y. Chumbimuni-Torres, Y. Xiang, R. Bash, P. Thavarungkul, P. Kanatharana, E. Pretsch, J. Wang, E. Bakker, *Anal. Chem.* **2008**, *80*, 707.
- [245] T. S. Pui, P. Kongsuphol, S. K. Arya, T. Bansal, *Sens. Actuators, B* **2013**, *181*, 494.
- [246] T. M. O'Regan, M. Pravda, C. K. O'Sullivan, G. G. Guilbault, *Talanta* **2002**, *57*, 501.
- [247] T. M. O'Regan, L. J. O'Riordan, M. Pravda, C. K. O'Sullivan, G. G. Guilbault, *Anal. Chim. Acta* **2002**, *460*, 141.
- [248] C. Siegmann-Thoss, R. Renneberg, J. F. C. Glatz, F. Spener, *Sens. Actuators, B* **1996**, *30*, 71.
- [249] A. Qureshi, J. H. Niazi, S. Kallempudi, Y. Gurbuz, *Biosens. Bioelectron.* **2010**, *25*, 2318.
- [250] Y. Wu, P. Xue, K. M. Hui, Y. Kang, *Biosens. Bioelectron.* **2014**, *52*, 180.
- [251] K. Y. Chumbimuni-Torres, Z. Dai, N. Rubinova, Y. Xiang, E. Pretsch, J. Wang, E. Bakker, *J. Am. Chem. Soc.* **2006**, *128*, 13676.
- [252] Y. Wang, Y. Zhou, J. Sokolov, B. Rigas, K. Levon, M. Rafailovich, *Biosens. Bioelectron.* **2008**, *24*, 162.
- [253] Y. Liu, N. Tuleouva, E. Ramanculov, A. Revzin, *Anal. Chem.* **2010**, *82*, 8131.
- [254] J.-D. Qiu, H. Huang, R.-P. Liang, *Microchimica Acta* **2011**, *174*, 97.
- [255] Q. Zhou, A. Rahimian, K. Son, D.-S. Shin, T. Patel, A. Revzin, *Methods* **2016**, *97*, 88.
- [256] H. V. Tran, B. Piro, S. Reisberg, L. D. Tran, H. T. Duc, M. C. Pham, *Biosens. Bioelectron.* **2013**, *49*, 164.
- [257] B. V. Chikkaveeraiah, V. Mani, V. Patel, J. S. Gutkind, J. F. Rusling, *Biosens. Bioelectron.* **2011**, *26*, 4477.
- [258] K. Hsieh, A. S. Patterson, B. S. Ferguson, K. W. Plaxco, H. T. Soh, *Angew. Chem.* **2012**, *124*, 4980.
- [259] Q. Zhou, D. Patel, T. Kwa, A. Haque, Z. Matharu, G. Stybayeva, Y. Gao, A. M. Diehl, A. Revzin, *Lab Chip* **2015**, *15*, 4467.
- [260] Q. Zhou, T. Kwa, Y. Gao, Y. Liu, A. Rahimian, A. Revzin, *Lab Chip* **2014**, *14*, 276.
- [261] C. Li, M. Curreli, H. Lin, B. Lei, F. N. Ishikawa, R. Datar, R. J. Cote, M. E. Thompson, C. Zhou, *J. Am. Chem. Soc.* **2005**, *127*, 12484.
- [262] K. V. Stepurska, O. O. Soldatkin, V. M. Arkhypova, A. P. Soldatkin, F. Lagarde, N. Jaffrezic-Renault, S. V. Dzyadevych, *Talanta* **2015**, *144*, 1079.
- [263] T. A. Sergeeva, A. P. Soldatkin, A. E. Rachkov, M. I. Tereschchenko, S. A. Piletsky, A. V. Elskaya, *Anal. Chim. Acta* **1999**, *390*, 73.
- [264] M. Magliulo, D. De Tullio, I. Vikholm-Lundin, W. M. Albers, T. Munter, K. Manoli, G. Palazzo, L. Torsi, *Anal. Bioanal. Chem.* **2016**, *408*, 3943.
- [265] K. Maehashi, T. Katsura, K. Kerman, Y. Takamura, K. Matsumoto, E. Tamiya, *Anal. Chem.* **2007**, *79*, 782.
- [266] M. Kamahori, Y. Ishige, M. Shimoda, *Biosens. Bioelectron.* **2007**, *22*, 3080.
- [267] T.-S. Pui, A. Agarwal, F. Ye, Y. Huang, P. Chen, *Biosens. Bioelectron.* **2011**, *26*, 2746.
- [268] J. Buth, A. Donner, M. Sachsenhauser, M. Stutzmann, J. A. Garrido, *Adv. Mater.* **2012**, *24*, 4511.
- [269] J. Buth, D. Kumar, M. Stutzmann, J. A. Garrido, *Appl. Phys. Lett.* **2011**, *98*, 76.
- [270] D. Elkington, N. Cooling, W. Belcher, P. C. Dastoor, X. Zhou, *Electronics* **2014**, *3*, 234.
- [271] X. Guo, A. Kulkarni, A. Doepke, H. B. Halsall, S. Iyer, W. R. Heineman, *Anal. Chem.* **2011**, *84*, 241.
- [272] K. Min, M. Cho, S.-Y. Han, Y.-B. Shim, J. Ku, C. Ban, *Biosens. Bioelectron.* **2008**, *23*, 1819.
- [273] P. Kongsuphol, H. H. Ng, J. P. Pursey, S. K. Arya, C. C. Wong, E. Stulz, M. K. Park, *Biosens. Bioelectron.* **2014**, *61*, 274.
- [274] C. Fenzl, T. Hirsch, O. S. Wolfbeis, *Angew. Chem., Int. Ed.* **2014**, *53*, 3318.
- [275] S. Mandal, J. M. Goddard, D. Erickson, *Lab Chip* **2009**, *9*, 2924.
- [276] Z. He, F. Tian, Y. Zhu, N. Lavlinskaia, H. Du, *Biosens. Bioelectron.* **2011**, *26*, 4774.
- [277] X. Liu, X. Song, Z. Dong, X. Meng, Y. Chen, L. Yang, *Biosens. Bioelectron.* **2017**, *91*, 431.
- [278] S. Jahns, M. Bräu, B. R.-O. Meyer, T. Karrock, S. R. B. Gutekunst, L. Blohm, C. Selhuber-Unkel, R. Buhmann, Y. Nazirizadeh, M. Gerken, *Biomed. Opt. Express* **2015**, *6*, 3724.
- [279] F. Vollmer, S. Arnold, *Nat. Methods* **2008**, *5*, 591.
- [280] Y. Gao, Z. Xin, B. Zeng, Q. Gan, X. Cheng, F. J. Bartoli, *Lab Chip* **2013**, *13*, 4755.

- [281] P. Chen, M. T. Chung, W. McHugh, R. Nidetz, Y. Li, J. Fu, T. T. Cornell, T. P. Shanley, K. Kurabayashi, *ACS Nano* **2015**, 9, 4173.
- [282] F. Vollmer, D. Braun, A. Libchaber, M. Khoshshima, I. Teraoka, S. Arnold, *Appl. Phys. Lett.* **2002**, 80, 4057.
- [283] A. M. Armani, R. P. Kulkarni, S. E. Fraser, R. C. Flagan, K. J. Vahala, *Science* **2007**, 317, 783.
- [284] H. A. Huckabay, S. M. Wildgen, R. C. Dunn, *Biosens. Bioelectron.* **2013**, 45, 223.
- [285] M. S. Luchansky, R. C. Bailey, *J. Am. Chem. Soc.* **2011**, 133, 20500.
- [286] P. Chen, N.-T. Huang, M.-T. Chung, T. T. Cornell, K. Kurabayashi, *Adv. Drug Delivery Rev.* **2015**, 95, 90.
- [287] J. Wang, D. Song, L. Wang, H. Zhang, H. Zhang, Y. Sun, *Sens. Actuators, B* **2011**, 157, 547.
- [288] J. Liu, M. A. Eddings, A. R. Miles, R. Bukasov, B. K. Gale, J. S. Shumaker-Parry, *Anal. Chem.* **2009**, 81, 4296.
- [289] M. Z. Mousavi, H.-Y. Chen, H.-S. Hou, C.-Y.-Y. Chang, S. Roffler, P.-K. Wei, J.-Y. Cheng, *Biosensors* **2015**, 5, 98.
- [290] H. Chen, Y. Hou, Z. Ye, H. Wang, K. Koh, Z. Shen, Y. Shu, *Sens. Actuators, B* **2014**, 201, 433.
- [291] E. Ouellet, C. Lausted, T. Lin, C. W. T. Yang, L. Hood, E. T. Lagally, *Lab Chip* **2010**, 10, 581.
- [292] I. Stojanović, T. J. G. van der Velden, H. W. Mulder, R. B. M. Schasfoort, L. W. M. M. Terstappen, *Anal. Biochem.* **2015**, 485, 112.
- [293] C. Cao, S. J. Sim, *Biosens. Bioelectron.* **2007**, 22, 1874.
- [294] A. Sonato, M. Agostini, G. Ruffato, E. Gazzola, D. Liuni, G. Greco, M. Travagliati, M. Cecchini, F. Romanato, *Lab Chip* **2016**, 16, 1224.
- [295] J. Martinez-Perdiguero, A. Retolaza, L. Bujanda, S. Merino, *Talanta* **2014**, 119, 492.
- [296] Y. Luo, F. Yu, R. N. Zare, *Lab Chip* **2008**, 8, 694.
- [297] H. J. Lezec, A. Degiron, E. Devaux, R. A. Linke, L. Martin-Moreno, F. J. Garcia-Vidal, T. W. Ebbesen, *Science* **2002**, 297, 820.
- [298] A. J. Haes, S. Zou, G. C. Schatz, R. P. Van Duyne, *J. Phys. Chem. B* **2004**, 108, 109.
- [299] M. D. Malinsky, K. L. Kelly, G. C. Schatz, R. P. Van Duyne, *J. Am. Chem. Soc.* **2001**, 123, 1471.
- [300] S. M. Yoo, D.-K. Kim, S. Y. Lee, *Talanta* **2015**, 132, 112.
- [301] K. M. Mayer, S. Lee, H. Liao, B. C. Rostro, A. Fuentes, P. T. Scully, C. L. Nehl, J. H. Hafner, *ACS Nano* **2008**, 2, 687.
- [302] G. K. Joshi, S. Deitz-McElyea, T. Liyanage, K. Lawrence, S. Mali, R. Sardar, M. Korc, *ACS Nano* **2015**, 9, 11075.
- [303] A. J. Haes, W. P. Hall, L. Chang, W. L. Klein, R. P. Van Duyne, *Nano Lett.* **2004**, 4, 1029.
- [304] B.-R. Oh, P. Chen, R. Nidetz, W. McHugh, J. Fu, T. P. Shanley, T. T. Cornell, K. Kurabayashi, *ACS Sensors* **2016**, 1, 941.
- [305] Y. Zhang, Y. Tang, Y.-H. Hsieh, C.-Y. Hsu, J. Xi, K.-J. Lin, X. Jiang, *Lab Chip* **2012**, 12, 3012.
- [306] H. Chen, X. Kou, Z. Yang, W. Ni, J. Wang, *Langmuir* **2008**, 24, 5233.
- [307] S. Lee, K. M. Mayer, J. H. Hafner, *Anal. Chem.* **2009**, 81, 4450.
- [308] C. Huang, K. Bonroy, G. Reekmans, W. Laureyn, K. Verhaegen, I. De Vlaminck, L. Lagae, G. Borghs, *Biomed. Microdevices* **2009**, 11, 893.
- [309] J. A. Ruennele, W. P. Hall, L. K. Ruvuna, R. P. Van Duyne, *Anal. Chem.* **2013**, 85, 4560.
- [310] L. J. Sherry, R. Jin, C. A. Mirkin, G. C. Schatz, R. P. Van Duyne, *Nano Lett.* **2006**, 6, 2060.
- [311] A. J. Haes, R. P. Van Duyne, *J. Am. Chem. Soc.* **2002**, 124, 10596.
- [312] B. Zhou, X. Xiao, T. Liu, Y. Gao, Y. Huang, W. Wen, *Biosens. Bioelectron.* **2016**, 77, 385.
- [313] K. M. Mayer, F. Hao, S. Lee, P. Nordlander, J. H. Hafner, *Nanotechnology* **2010**, 21, 255503.
- [314] Y. Song, P. Chen, M. T. Chung, R. Nidetz, Y. Park, Z. Liu, W. McHugh, T. T. Cornell, J. Fu, K. Kurabayashi, *Nano Lett.* **2017**, 17, 2374.
- [315] R. Fan, O. Vermesh, A. Srivastava, B. K. H. Yen, L. Qin, H. Ahmad, G. A. Kwong, C.-C. Liu, J. Gould, L. Hood, *Nat. Biotechnol.* **2008**, 26, 1373.
- [316] Q. Han, N. Bagheri, E. M. Bradshaw, D. A. Hafner, D. A. Lauffenburger, J. C. Love, *Proc. Natl. Acad. Sci. USA* **2012**, 109, 1607.
- [317] Y. Liu, T. Kwa, A. Revzin, *Biomaterials* **2012**, 33, 7347.
- [318] E. Sinkala, E. Sollier-Christen, C. Renier, E. Rosàs-Canyelles, J. Che, K. Heirich, T. A. Duncombe, J. Vlassakis, K. A. Yamauchi, H. Huang, S. S. Jeffrey, A. E. Herr, *Nat. Commun.* **2017**, 8, 14622.
- [319] M. P. Landry, H. Ando, A. Y. Chen, J. Cao, V. I. Kottadiel, L. Chio, D. Yang, J. Dong, T. K. Lu, M. S. Strano, *Nat. Nanotechnol.* **2017**, 12, 368.